

INVESTIGATING THE ROLE OF mTOR SIGNALING AS A POINT OF CONVERGENCE  
FOR AUTISM RISK GENES

by

Christy LaFlamme

A Thesis Submitted to the Faculty of  
The Harriet L. Wilkes Honors College  
in Partial Fulfillment of the Requirements for the Degree of  
Bachelor of Science in the Biological and Physical Sciences  
with a Major Concentration in Biological Chemistry  
and Minor Concentration in Mathematics

Wilkes Honors College of  
Florida Atlantic University

Jupiter, Florida

May 2020

Investigating the role of mTOR signaling as a point of convergence for autism risk genes

by

Christy LaFlamme

This thesis was prepared under the direction of the candidate's research advisor, Dr. Damon Page, and the candidate's thesis advisors, Dr. Chitra Chandrasekhar and Dr. Catherine Trivigno, and has been approved by the members of her supervisory committee. It was submitted to the faculty of the Honors College and was accepted in partial fulfillment of the requirements for the degree of Bachelor of Science in the Biological and Physical Sciences.

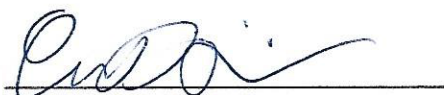
SUPERVISORY COMMITTEE:



Dr. Damon Page, Scripps Research



Dr. Chitra Chandrasekhar, Wilkes Honors College



Dr. Catherine Trivigno, Wilkes Honors College

---

Dean Timothy Steigenga, Wilkes Honors College

---

Date

## Acknowledgements

I would like to express my sincere gratitude to all of the members of the Page laboratory at Scripps Research for academic direction and support of this research project. Thank you, Dr. Damon Page, for welcoming me into your laboratory, enlightening me to the ways of neuroscience, preparing me to pursue a research career, and always keeping your office door open, whether to discuss my ongoing experiments or life outside the lab. You are an inspiration to all of us. Thank you to graduate student mentor, Jenna Levy, for teaching me how to perform various experiments described in this manuscript, putting up with my mistakes, and pushing me to grow in my independence as a scientist. You are truly an exceptional mentor and a great friend. Thank you to Dr. Ori Cohen “co-colleague helper” for mentoring me in primary neuronal culture techniques. These experiments would not have been possible without you. Thank you also to laboratory members Aya Zucca, Dr. Amy Clipperton-Allen, and Niki Mabie for your help, advice, and warmth during my time here. My experience in the Page laboratory as a Biomedical Laboratory Experience for Undergraduates (BLEU) student was made possible by Rosie Zeckler, Scripps Research Education Outreach Coordinator. Thank you, Rosie, for helping me to navigate my undergraduate research journey.

I want to thank my wonderful honors college thesis advisors, Dr. Chitra Chandrasekhar and Dr. Catherine Trivigno, for guidance of this thesis project and continued mentorship throughout my time at the Harriet L. Wilkes Honors College. Dr. C, thank you for serving as the best honors college advisor I could have ever asked for. I have learned so much from my time spent in your classes and in your office. You have changed my perspective of the world and how science works within it. Dr. Trivigno, thank you for being one of the most genuine, caring, helpful, understanding, and supportive individuals I have ever met in my life. I am honored to have been a part of your legacy at Florida Atlantic University, and I hope to continue that legacy as an alumnus.

I am also very grateful to have had the opportunity to work with Dr. Yaouen Fily on the computational analysis described here. In an attempt to integrate my passion for the biomedical sciences with my love for mathematics, I have uncovered newfound interests in computer programming. Thank you, Dr. Fily, for giving me valuable skills that will serve me well in graduate school and beyond.

## **ABSTRACT**

Author:	Christy LaFlamme
Title:	Investigating the role of mTOR signaling as a point of convergence for autism risk genes
Institution:	The Harriet L. Wilkes Honors College of Florida Atlantic University
Thesis Advisors:	Dr. Damon Page and Dr. Chitra Chandrasekhar
Degree:	Bachelor of Science in the Biological and Physical Sciences
Major Concentration:	Biological Chemistry
Minor Concentration:	Mathematics
Year:	2020

Subsets of children with Autism Spectrum Disorder (ASD) display alterations in brain growth that are heavily influenced by genetic risk factors. For instance, mutations in *PTEN*, a canonical regulator of the mTOR growth signaling pathway, determine macroscale brain size. Mutations in *DYRK1A* disrupt many important neurodevelopmental processes resulting in severe morphological and behavioral consequences. Yet, the cellular and molecular mechanisms governing these alterations remain unclear. Previous work in the laboratory suggests that *Dyrk1a* deficiency is sufficient to cause cortical growth deficits and potentially decrease mTOR growth signaling. We hypothesize that *Dyrk1a* deficiency causes neuronal undergrowth via downregulated mTOR signaling and that pharmacological activation of the mTOR pathway will rescue this phenotype. To investigate this, we cultured primary cortical neurons from a conditional *Dyrk1a* mouse model and performed Sholl analysis on stained neurons to characterize neuronal morphology. Our results support mTOR as point of convergence for autism risk genes and (1-3)IGF-1 as a potential therapeutic for *DYRK1A* deficiencies and related disorders. Future work will investigate *PTEN* deficient neurons in culture to further elucidate the molecular intersections of this pathway.

## Table of Contents

Introduction .....	1
Autism Spectrum Disorder .....	1
The Convergence of Autism Risk Genes .....	2
<i>PTEN</i> and Macrocephaly .....	3
<i>DYRK1A</i> and Microcephaly .....	4
The mTOR Growth Signaling Pathway .....	5
<i>DYRK1A</i> and mTOR Signaling .....	6
Insulin-like Growth Factor-1 (IGF-1) .....	7
(1-3)IGF-1: Active Peptide of IGF-1 .....	9
Aims .....	9
Aim 1: Characterize the effects of <i>Dyrk1a</i> mutation on neuronal morphology in primary neuronal culture.....	9
Aim 2: Rescue the neuronal phenotype of <i>Dyrk1a</i> mutants in culture with (1-3)IGF-1 treatment .....	9
Aim 3: Write a novel Python code to automate neurite analysis .....	10
Materials and Methods .....	11
Animals and tissue collection .....	11
Primary neuronal culture .....	12
Drug treatment .....	12
Immunocytochemistry .....	13
Microscopy and Imaging .....	13
Image analysis .....	14

Statistical analysis .....	14
Computational analysis .....	15
Results and Discussion .....	15
Sholl analysis of cHET versus control neurons .....	15
Sholl analysis of cHET versus control neurons after treatment with (1-3)IGF-1 .....	18
Phosphorylated S6 kinases as a readout of mTOR activity in culture .....	21
Python code written to automate Sholl analysis .....	21
Conclusion .....	24
Future Work .....	25
References .....	26
Supplementary Figures .....	33
Code Appendix .....	37
Code Appendix A: <tuj1_p-s6_workflow.ijm> .....	37
Code Appendix B: <tuj1_p-s6_workflow.ipynb>.....	38

## List of Figures

<b>Figure 1:</b> Autism risk gene <i>DYRK1A</i> is critical for neurodevelopment .....	2
<b>Figure 2:</b> DYRK1A may regulate mTOR growth signaling .....	5
<b>Figure 3:</b> Generation of conditional <i>Dyrk1a</i> mutants .....	8
<b>Figure 4:</b> Summary of experimental workflow .....	10
<b>Figure 5:</b> Primary neuronal culture and immunostaining .....	16
<b>Figure 6:</b> Conditional <i>Dyrk1a</i> mutant neurons exhibit altered neuronal morphology .....	17
<b>Figure 7:</b> Neuronal morphology of conditional <i>Dyrk1a</i> mutant neurons can be rescued by (1-3)IGF-1 .....	19
<b>Figure 8:</b> <i>Dyrk1a</i> cHet neurons display deficits in neuronal morphology that can be rescued by (1-3)IGF-1 .....	20
<b>Supplementary Figure 1:</b> A comparison of Sholl analysis methods—workflow .....	33
<b>Supplementary Figure 2:</b> Mathematical representation of Sholl intersections in Python ..	32
<b>Supplementary Figure 3:</b> A comparison of Sholl analysis methods—output .....	35
<b>Supplementary Figure 4:</b> A comparison of Sholl analysis methods—neurite trace .....	36

## Introduction

### Autism Spectrum Disorder

Autism spectrum disorder (ASD) encompasses a range of highly heritable neurodevelopmental disorders and affects 1 in 59 children, approximately 1 in 37 boys and 1 in 151 girls, in the United States (Baio et al., 2018). ASD is characterized by social impairments and repetitive behaviors resulting from genetic and non-genetic risk factors as depicted in **Figure 1A** (American Psychiatric Association. & American Psychiatric Association. DSM-5 Task Force., 2013). This heterogenous grouping of syndromes is usually hallmarked by a difficulty communicating with others during early childhood and continues to manifest itself in the form of social and physical impairments well into adulthood (Park et al., 2016). Since ASD is representative of a variety of related disorders with overlapping or similar symptoms, a unitary molecular, cellular, or systems cause is unknown (Geschwind, 2008). However, subsets of individuals with ASD display alterations in brain growth that are heavily influenced by mutations in autism risk genes. Progress in the field of autism research at the genetic, neurodevelopmental, and cognitive levels provides insight into risk factors which may be used as biological markers to better categorize and subsequently diagnose ASD. Furthermore, unraveling the mechanisms underlying disrupted brain growth may suggest novel molecular targets for the development of therapies to rescue the social deficits or physical impairments observed in ASD patients.

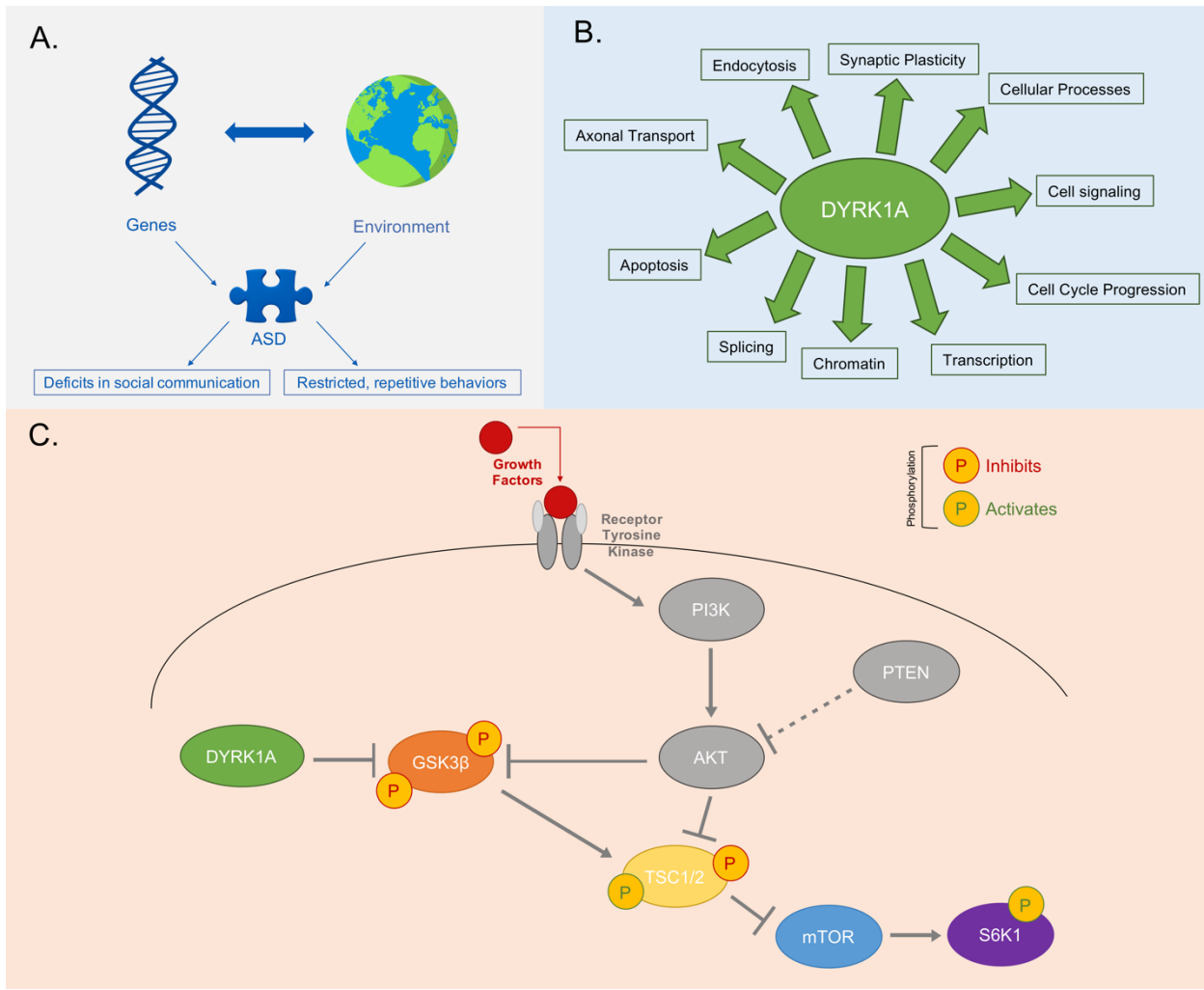


**Figure 1:** Autism risk gene *DYRK1A* is critical for neurodevelopment. **A.** Autism Spectrum Disorder (ASD) is influenced by genetic and environmental factors. **B.** *DYRK1A* functional roles include important genetic, cellular, and systems-level processes. **C.** *DYRK1A* may act on the mTOR signaling cascade through inhibitory phosphorylation of GSK3 $\beta$ .

### The Convergence of Autism Risk Genes

Given the heterogeneity of the ASD, it is not uncommon that autism risk genes converge on common pathways (Geschwind, 2008). The mechanistic target of rapamycin (mTOR) signaling pathway is critical for mammalian growth and development, and dysregulations of mTOR have been linked to cellular mechanisms underlying disorders on the autism spectrum (Rosina et al.,

2019; Sato, 2016; Winden, Ebrahimi-Fakhari, & Sahin, 2018). The overarching goal of this project is to provide a deeper understanding of how autism risk genes, specifically *phosphatase and tensin homolog* (*PTEN*) and *dual-specificity tyrosine-(Y)-phosphorylation-regulated kinase 1 A* (*DYRK1A*), may converge on mTOR signaling to regulate neuronal development of the cerebral cortex and how dysregulation shapes neuronal morphological deficits consistent with ASD.

### *PTEN* and Macrocephaly

Macrocephaly, an enlargement of the head and brain, has been reported in autistic children since ASD was first observed (Kanner, 1943). Mutations in *PTEN* are associated with approximately 10% of all macrocephalic (OMIM #605309) ASD cases (Frazier et al., 2015). *PTEN* encodes negative regulators of the PI3K-Akt-mTOR pathway (Cully, You, Levine, & Mak, 2006), which are important for cell growth and protein synthesis (Laplante & Sabatini, 2012). Hence, when *PTEN* is mutated, cell number and size are both increased, and macrocephaly can result. This overgrowth appears to be driven by hyperplasia with excess neurons at birth and excess glia in adulthood as demonstrated by previous work with mice (Chen, Huang, Séjourné, Clipperton-Allen, & Page, 2015). Germline haploinsufficient *Pten<sup>+/−</sup>* mice exhibit dysregulation of mTOR signaling and characteristics of brain hyperconnectivity such as increased axonal branching and synaptic bouton density on medial prefrontal cortical (mPFC) neurons projecting to the basolateral amygdala (BLA) (W.-C. Huang, Chen, & Page, 2016). Suppression of mTOR in *Pten* haploinsufficient mice has been shown to rescue both synaptic and social deficits (W. C. Huang, Chen, & Page, 2019). Given that mTOR is at the intersection of many important processes, it is likely that various autism risk genes converge on mTOR and related signaling cascades. Yet, these genetically encoded molecular crossroads are sparsely reported.

### DYRK1A and Microcephaly

Dual-specificity tyrosine-(Y)-phosphorylation-regulated kinase 1 A (DYRK1A) is a tyrosine and serine/threonine kinase implicated in neurodevelopment and brain function (Becker & Sippl, 2011). With important roles in apoptosis, cell signaling, axonal transport cytoskeleton dynamics, and synaptic plasticity (**Figure 1B**), DYRK1A activation must be tightly regulated (Arbones, Thomazeau, Nakano-Kobayashi, Hagiwara, & Delabar, 2019). Otherwise, neurodevelopmental and neurodegenerative diseases may arise. Previously, *DYRK1A* haploinsufficiency has been linked to intellectual disability (ID) in individuals with *de novo* heterozygous variants of *DYRK1A* (Ji et al., 2015). Patients exhibited congenital microcephaly, developmental delay, and social impediments. Similarly, Autistic-like features have been reported in *Dyrk1a* haploinsufficient mice (Arranz et al., 2019; Fotaki et al., 2002; Raveau, Shimohata, Amano, Miyamoto, & Yamakawa, 2018). It has been proposed that autosomal dominant mental retardation MRD7 (OMIM #614104) is caused by *DYRK1A* heterozygous abnormalities (Courcet et al., 2012) further linking *DYRK1A* disruption to microcephaly (B. W. M. van Bon, Coe, de Vries, & Eichler, 1993). Mutations in *DYRK1A* have been recognized as a risk factor leading to a syndromic form of ASD and ID (B. W. van Bon et al., 2016). At the molecular level, DYRK1A is involved in ERK/AKT and GSK3 $\beta$  activation (Abekhoukh et al., 2013; Scales, Lin, Kraus, Goold, & Gordon-Weeks, 2009), both of which are key players in the mTOR pathway (Ma & Blenis, 2009). While it is not fully understood whether or not DYRK1A regulates mTOR signaling directly, DYRK1A can be connected to mTOR through established mechanisms of action, notably DYRK1A inhibitory phosphorylation of GSK3 $\beta$ , a known regulator of mTOR signaling. Recent data from the laboratory suggests that *Dyrk1a* may impinge on the mTOR pathway via the proposed mechanism shown in **Figure 1C** and simplified in **Figure 2A**, further recapitulating the

finding that inactivation of mTOR in the developing brain, likewise, causes microcephaly (Cloetta et al., 2013).

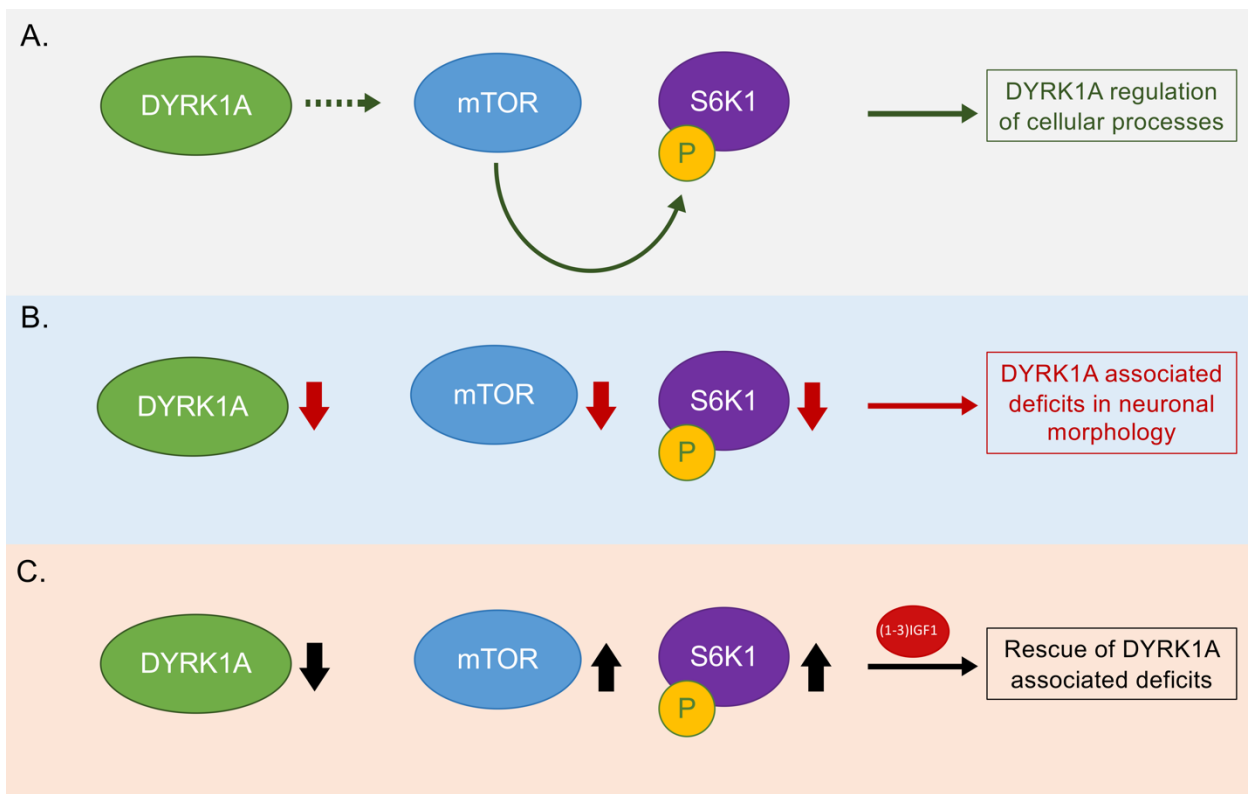


**Figure 2:** DYRK1A may regulate mTOR growth signaling. **A.** DYRK1A is proposed to act on mTOR growth signaling to carry out cellular processes. **B.** DYRK1A deficiency may potentially decrease mTOR signaling. **C.** (1-3)IGF-1 is expected to rescue effects of DYRK1A deficiency.

#### The mTOR Growth Signaling Pathway

The mechanistic target of rapamycin (mTOR) signaling pathway detects and responds to external signals to regulate growth and homeostasis in living organisms (Laplante & Sabatini, 2012) as well as protein synthesis. As such, mTOR is responsible for controlling a wide array of critical processes that generate and use energy, such as the insulin signaling pathway (Laplante & Sabatini, 2012). This serine/threonine protein kinase belongs to the phosphoinositide 3-kinase

(PI3K)-related kinase family and forms two major complexes, mTORC1 and mTORC2 (Ma & Blenis, 2009). While mTORC1 is largely implicated in protein synthesis and cell growth, mTORC2 regulates survival and metabolism (Laplante & Sabatini, 2012). The importance of properly regulated mTOR growth signaling is underscored by the various neurological diseases and disorders associated with its dysregulation, including autism (Lipton & Sahin, 2014; Saxton & Sabatini, 2017; Winden et al., 2018; Wong, 2013). While it may be inferred that *PTEN* and *DYRK1A* are implicated in a common pathway directly or indirectly, characteristics of the relationship between these genes with respect to mTOR have been largely unexplored. As previously mentioned, *PTEN* is a known negative regulator of mTORC1 (Sulis & Parsons, 2003), but it is unclear if *DYRK1A* impinges directly on mTORC1. The goal of this research is to provide a better understanding of the convergence of these autism risk genes on mTOR signaling to regulate neuronal development.

### DYRK1A and mTOR Signaling

Previous investigations of *Dyrk1a* *in vivo* analyze germline mutations or total knockdown of *Dyrk1a* in mice (Arranz et al., 2019; Fotaki et al., 2002; Martinez de Lagran et al., 2012; Raveau et al., 2018). These mice exhibit severe undergrowth systemically (Fotaki et al., 2002) and thus are not ideal for isolating the effects of *Dyrk1a* on brain function. Cre-Lox recombination, as illustrated in **Figure 3A**, can be used to excise genes in a tissue specific manner and thereby eliminate the negative effects of genetic mutations on the periphery. Cortex specific *Emx1-Cre* (Gorski et al., 2002) conditional *Dyrk1a* heterozygous (cHet) mice are highly relevant to autism, since the cortex is responsible for social interaction, and serve as an important tool for the investigation of *Dyrk1a* on brain growth without the negative effects of removing the gene from

all tissues. These *Dyrk1a* cHet mice can be generated via an optimized cross shown in **Figure 3B**. Herein, it is hypothesized that neurons cultured from *Dyrk1a* conditional heterozygotes will exhibit characteristics of neurite underdevelopment, such as deficits in neurite complexity, due to decreased mTOR activity (**Figure 2B**) and that increasing mTOR signaling will be able to rescue *Dyrk1a* mutant phenotype (**Figure 2C**). Since mTOR directly phosphorylates S6 kinases, phosphorylated S6 (p-S6) kinases should be synonymous as readout for mTOR activity in culture.

### Insulin-like Growth Factor-1 (IGF-1)

Insulin-like growth factor-1 (IGF-1) is known mediator of the mTOR signaling cascade. Endogenous IGF-1 binds IGF-1 receptor to initiate intracellular signaling, which includes the activation of PI3K-Akt-mTOR and Ras-MEK1/2-ERK1/2 pathways (Laplante & Sabatini, 2012). Previously, IGF-1 has been shown to rescue Rett syndrome, an autism spectrum disorder, phenotypes in mice by increasing synaptic signaling pathway proteins, re-establishing cortical excitatory synaptic transmission, and restoring dendritic spine density (Castro et al., 2014). These mice have mutated *Mecp2*, which leads to downregulation of mTOR signaling in a similar manner to what is hypothesized for *Dyrk1a*. Further, IGF-1 is an FDA approved drug, injection known as Mecasermin, for use in children with short stature or severe undergrowth (Bang, Polak, Woelfle, Houchard, & Group, 2015; Ratner, 2005).

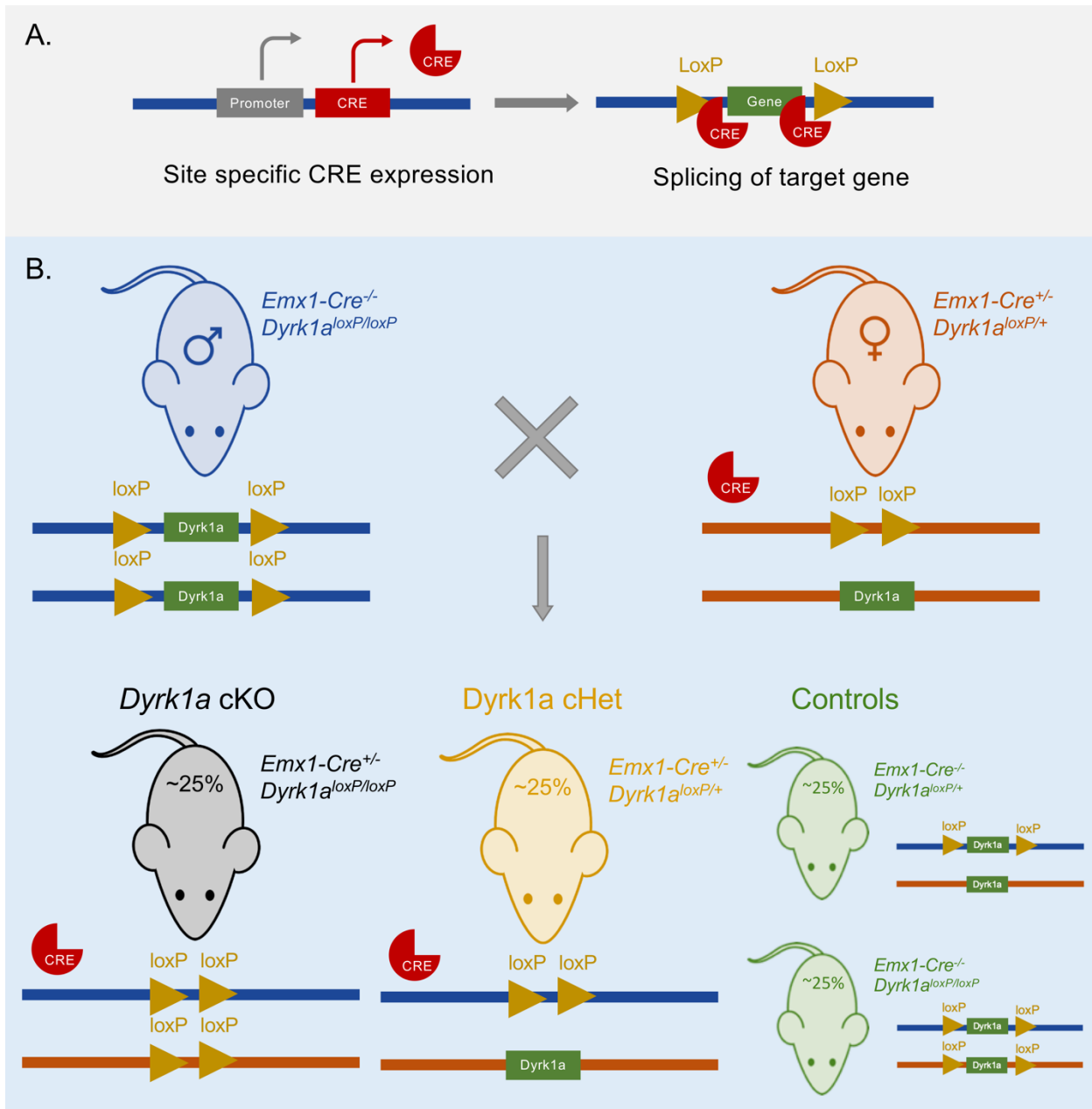


**Figure 3:** Generation of conditional *Dyrk1a* mutants. **A.** Schematic of the Cre-lox recombination system used to generate *Dyrk1a* conditional heterozygous (cHet) mice. **B.** Schematic of genetic cross approach. cHet mice (*Emx1-cre<sup>+/-</sup>*; *Dyrk1a<sup>loxP/+</sup>*) and control mice (*Emx1-cre<sup>+/-</sup>*; *Dyrk1a<sup>loxP/+</sup>* or *Dyrk1a<sup>loxP/loxP</sup>*) collected at P0 for primary neuronal culture. cKO = conditional knockout. cHet = conditional heterozygote.

### (1-3)IGF-1: Active Peptide of IGF-1

Endogenous truncated analogue of IGF-1, or (1-3)IGF-1, has the N-terminal tripeptide (Gly-Pro-Glu) omitted, considerably decreasing binding affinity for insulin-like growth factor binding proteins (IGFBPs) that can inhibit biological activity (Ross, Francis, Szabo, Wallace, & Ballard, 1989). This affords (1-3)IGF-1 an approximately 10-fold greater potency versus IGF-1 at stimulating hypertrophy and proliferation of cultured cells (Ballard, Wallace, Francis, Read, & Tomas, 1996). The (1-3)IGF-1 active peptide indirectly activates IGF-1 receptor by acting through IGF-1, therefore triggering the same signaling cascades (Corvin et al., 2012). Recently, ACADIA Pharmaceuticals initiated a Phase 3 clinical trial of (1-3)IGF-1, known as Trofinetide, to treat Rett syndrome. Thus, successful rescue of *Dyrk1a* mutant phenotype with (1-3)IGF-1 could eventually lead to the repurposing of the drug for autism patients with *DYRK1A* mutations and related disorders.

### **Aims**

#### **Aim 1:** Characterize the effects of *Dyrk1a* mutation on neuronal morphology in primary neuronal culture

The first aim of this project is to characterize neurite arborization of individual neurons from *Dyrk1a* primary neuronal cultures via Sholl analysis, a measure of neuronal complexity.

#### **Aim 2:** Rescue the neuronal phenotype of *Dyrk1a* mutants in culture with (1-3)IGF-1 treatment

Upon establishing a neurite phenotype of mutant *Dyrk1a* cHet neurons, the second aim of this project is to attempt a rescue of *Dyrk1a* mutant neuronal arborization via treatment with (1-3)IGF-1 to upregulate mTOR signaling (Ballard et al., 1996; Corvin et al., 2012). A graphical summary of aims 1 and 2 is depicted in **Figure 4**.

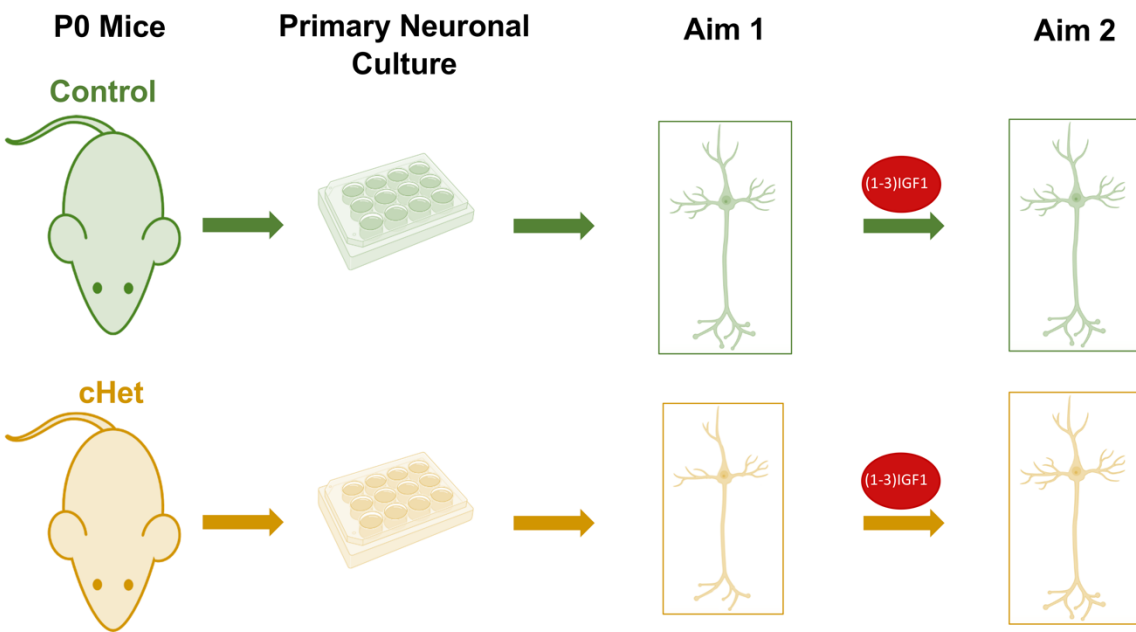


**Figure 4:** Summary of experimental workflow. Graphical summary of experimentation and analysis. Generation of conditional *Dyrk1a* deficient mice, maintenance of primary neuronal culture, analysis of neuronal morphology via Sholl analysis, and treatment with (1-3)IGF-1 to attempt a rescue *Dyrk1a* mutant phenotype.

#### Aim 3: Write a novel Python code to automate neurite analysis

To obtain greater control over datasets and expedite future analyses, a final aim of this study is to write a novel python code to automate Sholl analysis.

## Materials and Methods

**Animals and tissue collection.** To excise *Dyrk1a* in a tissue specific manner, the Cre-Lox recombination system (**Figure 3A**) was used to generate a conditional heterozygous deletion of *Dyrk1a* in the mouse cerebral cortex. *Emx1-Cre* mice (JAX stock #005628) were previously purchased from Jackson Laboratories and backcrossed for at least six generations with *Dyrk1a* floxed mice. In order to generate *Emx1-Cre* conditional heterozygous *Dyrk1a* mice, male (*Emx1-Cre*<sup>-/-</sup>; *Dyrk1a*<sup>loxP/loxP</sup>) and female (*Emx1-Cre*<sup>+/+</sup>; *Dyrk1a*<sup>loxP/+</sup>) C57BL/6J mice were bred as depicted in **Figure 3B**. Cages were monitored throughout the period of gestation, and pups were collected at postnatal day zero (P0). Genotypes of pups were confirmed by polymerase chain reaction (PCR) of DNA extracted from mice tails. Tail samples from P0 pups were each placed in 75 µL of basic solution (0.025N NaOH, 2 mM EDTA). The samples were cycled through the thermocycler and then neutralized with an equal volume of neutralizing solution (50 mM Tris-HCl). DNA (1 µL) was combined with appropriate primers (*Universal Cre*, *Emx-1 Cre*, and *Dyrk1a*) and OneTaq® Hot Start 2X Master Mix with Standard Buffer (#M0484). Samples were run through PCR cycling and then quenched with Thermo Scientific 6X loading dye (#R1161) before resolving on a 2% agarose gel with EtBr for 35 minutes at 140 V. The gel was imaged and analyzed on an AlphaImager® HP. Conditional heterozygous mouse samples were matched with samples from control littermates, and sex was randomly selected in each genotype. All procedures were performed in accordance with the National Institutes of Health Guide for the Care and Use of Laboratory Animals and approved by the Scripps Research Institutional Animal Care and Use Committee.

**Primary neuronal culture.** Brains from P0 mice were removed, and whole cortices were dissected. Individual cortices were placed into 1 mL chilled dissecting media (1X HBSS (14175-095), 30 mM glucose, 60 µM HEPES). After aspiration of the dissecting media, the tissue was enzymatically dissociated with papain (LS003126) that was previously diluted 1:80 in pre-warmed plating media (Neurobasal A (10888-022), 5% FBS (16000044), and 1% penicillin/streptomycin (p/s) / 0.25% glutamine (10378-016)) and incubated at 37 °C for 15 minutes. The papain was removed, and the tissue was pipetted into a single-cell suspension in plating media. The suspensions were filtered using 40 µm nylon cell strainers (Fischer Scientific, #352340), and the filtered suspension was centrifuged at 280 RCF for 5 minutes. The supernatant was aspirated, and the pellet was re-suspended in pre-warmed plating media. Samples of the suspensions were diluted 1:4 in trypan blue, and cells were counted with a manual hemocytometer for determination of sample concentration. The cells were then plated at 50,000 cells per well in sterile 12-well plates (#07-200-82) containing Poly-D-Lysine (PDL) coated coverslips (GG-18-pdl). At the first day-in-vitro (DIV0), the plating media was fully exchanged with 1 mL feeding media (Neurobasal A, 1% Penicillin/Streptomycin/0.25% glutamine, 2% B-27™ serum-free supplement (17504-044)). At DIV3, the volume of feeding media was doubled by adding 1 mL of feeding media to all wells, and at every three DIV, 1 mL of media was replaced with 1 mL fresh feeding media until DIV15. Cells were washed with 1X PBS and fixed at DIV15 with 4% paraformaldehyde (PFA) in 1X PBS for 10 minutes at room temperature. After undergoing three additional washes in 1X PBS to remove remaining PFA, cells were stored in PBS at 4 °C until further use.

**Drug treatment.** Primary neurons were dosed with either Milli-Q water as vehicle or 100 ng/mL of (1-3)IGF-1 (Art. No. 40261041000; CAS No. 32302-76-4) dissolved in Milli-Q water as drug,

both sterilized with the Steriflip® Vacuum Driven Filtration System. Cells were dosed by removing 1 mL feeding media and adding 1 mL of vehicle or drug diluted in feeding media for three consecutive days with 24-hour incubation periods in between each dose and a 12-hour incubation period between the final dose and fixation of the cells at DIV15.

**Immunocytochemistry.** Cells were washed in PBS washing solution (1X PBS supplemented with 0.1% Triton) and then blocked in PBS blocking solution (1X PBS supplemented with 0.1% Triton and 1% BSA) for 1 hour at room temperature. Cells were incubated with primary antibodies overnight at 4°C in a humidity chamber. Primary antibodies were diluted as follows: Ms Tuj1 (1:750, #ab78078); Rb Phospho-S6 (1:1000, #2211); Rt Ctip2 (1:1000, #ab18465). Tuj1 is a beta tubulin marker that fills neurons; phospho-S6 is indicative of phosphorylated S6 kinases; and Ctip2 is enriched in layer V neurons. The following day, cells were washed in PBS washing solution three times with 20 minutes for each wash prior to incubation at room temperature with 1:1000 horseradish peroxidase (HRP)-linked IgG (H+L) cross-adsorbed secondary antibodies as follows: Goat anti-Mouse, 488 (#A11001), Donkey anti-Rabbit, 594 (#A21207), Goat anti-Rat, 647 (#A21247). The secondary antibodies were diluted in PBS blocking solution and incubated with the cells for 1 hour at room temperature. After washing with 1X PBS, the coverslips were removed from the wells and allowed to dry for 5 minutes before being mounted onto slides (48311-703) with mounting medium containing DAPI (Life Technologies #P36935), a DNA marker.

**Microscopy and Imaging.** All coverslip images were taken at 40X magnification on an Olympus VS-120 epifluorescence microscope. The associated channel of the secondary antibody and the microscope exposure time used is as follows: Tuj1 (488 nm, FITC 100 ms); Phospho-S6 (594 nm,

TRITC 200 ms); Ctip2 (647 nm, CY5 300 nm). The microscope was focused manually in 488 nm, FITC 100 ms; images were processed by VS-Desktop software; and files were exported as RGB TIFF images.

**Image analysis.** All coverslip images were analyzed with Fiji ImageJ software (Schindelin et al., 2012). The Simple Neurite Tracer (SNT) plugin was used to draw neurite traces for individual neurons. Sholl analysis was run using plugins that come pre-installed with Fiji ImageJ. The Sholl analysis plugin was used to run Sholl analysis on the reconstructed neurite traces after thresholding images to a binary format. An ImageJ macro <.ijm> of this workflow was created with the ImageJ Macro (IJM) built-in recorder functionality. IJM is a simple programming language that can be used to create a text-file documents instructing ImageJ to carry out a series of commands. The <.ijm> analysis workflow for DIV15 50,000 Tuj1, p-S6, and Ctip2 stained neurons <tuj1\_p-s6\_workflow.ijm> can be found in **Code Appendix A**.

**Statistical analysis.** A minimum of 3 mice per genotype and approximately 30-35 neurons per mouse were analyzed in this study. Both sexes were taken into account since relatively no sexual dimorphisms were reported in current molecular *Dryk1a* studies of the laboratory. Raw data was statistically analyzed in Microsoft Excel and plotted in GraphPad Prism. A 2-way ANOVA (genotype and drug) was used to statically compare vehicle versus drug treatment for both genotypes. A 3-way ANOVA (genotype, drug, and distance) was used to statistically evaluate vehicle versus drug treatment from both genotypes at various distances from the soma. After significant interaction was determined, *post hoc* two tailed student *t*-test were used to assess the significance between individual group pairs.

**Computational analysis.** Python code was written to automate Sholl analysis and more efficiently handle the data. The most recent version of Python (3.7.2) for Macintosh was installed on a MacBook Pro. All Python code was written in Jupyter Notebooks, a Project Jupyter integrated development environment (IDE) that allows for live code, visualizations, and narrative text. Modules used in the Python code include [glob], [os], [sys], [shutil], [cv2], [ijroi], [numpy], [matplotlib.pyplot], and [pandas]. The workflow for the Python code versus ImageJ analysis is depicted in **Supplemental Figure 1** and more deeply described in the following section. The Python code <tuj1\_p-s6\_workflow.ipynb> as written in Jupyter Notebook can be found in **Code Appendix B.**

## Results and Discussion

### Sholl analysis of cHet versus control neurons

In this study, primary cortical neurons from a *Dyrk1a* mouse model of autism were cultured until DIV15. Primary neuronal cultures were then stained with various antibodies via immunocytochemistry (ICC), a technique used to visualize the cellular landscape. A schematic of the primary neuronal culture and immunocytochemistry workflow is shown in **Figure 5**. Since DYRK1A is hypothesized to act on mTOR signaling, a key regulatory pathway of cellular growth, neuronal morphology of individual neurons was investigated. Sholl analysis, the measure employed here to characterize neurite arborization, is a method in which the number of intersections at a specific distance from the soma is plotted as a curve. The greater the number of intersections at each distance indicates a greater degree of neuronal complexity.

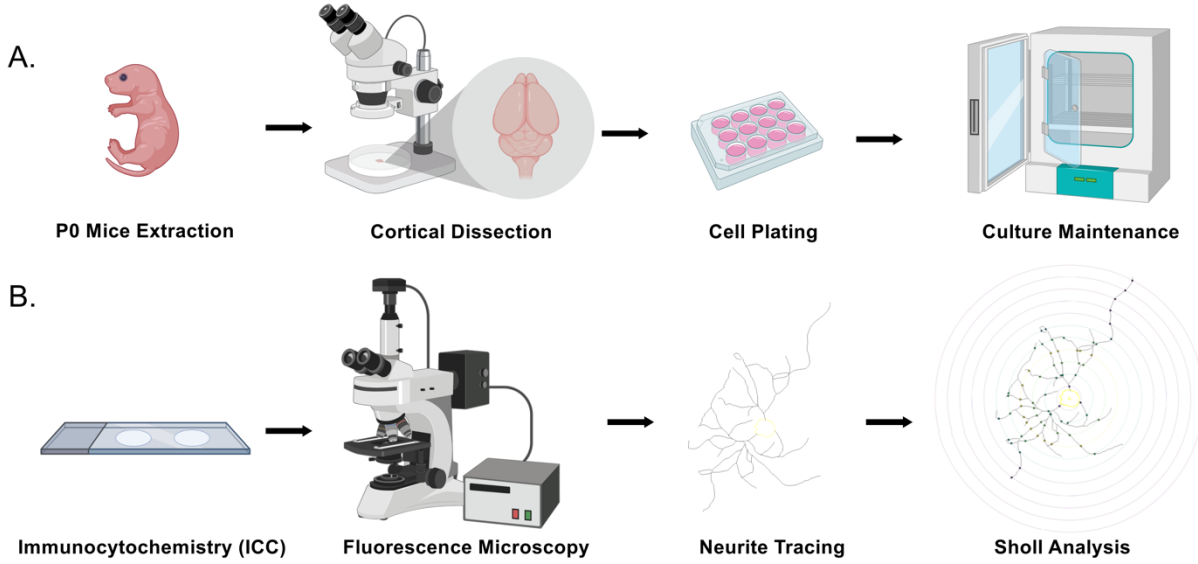


**Figure 5:** Primary neuronal culture and immunostaining. **A.** Schematic of primary neuronal culture workflow. Mice collected, cortices dissected, and cells plated at P0/DIV0. Cells maintained in culture until DIV15 (fixed with 4% PFA). **B.** Neurons visualized using immunocytochemistry. VS-120 microscope used to take images of specimens. Neurite traces hand-drawn with Fiji ImageJ SNT. Sholl profile for individual neurons obtained from Fiji ImageJ Sholl plugin. Images shown in **A.** and **B.** adapted from BioRender scientific illustration tools. Example neurite trace rendered from ImageJ.

Since *Dyrk1a* is expressed throughout brain development and responsible for a variety of neuronal growth processes, it was expected that a cortex-specific heterozygous mutation of *Dyrk1a* would lead to *in cellulis* deficits in neuronal morphology. Sholl analysis of neurite arborization on individual cultured neurons (**Figure 6A**) indicates a significant decrease in neurite complexity of *Dyrk1a* cHet mice as compared to control mice (**Figure 6B**). A 2-way ANOVA (genotype and drug) on area under the curve (AUC) data from Sholl plot with Tukey's multiple comparisons test shows a significant interaction between genotype and drug treatment ( $F_{1,8}=5.309, P=0.0477$ ). These

data align with the mechanism of action proposed here in addition to previous reports of *Dyrk1a* deficiency in culture (Dang et al., 2018; Martinez de Lagran et al., 2012; Scales et al., 2009).

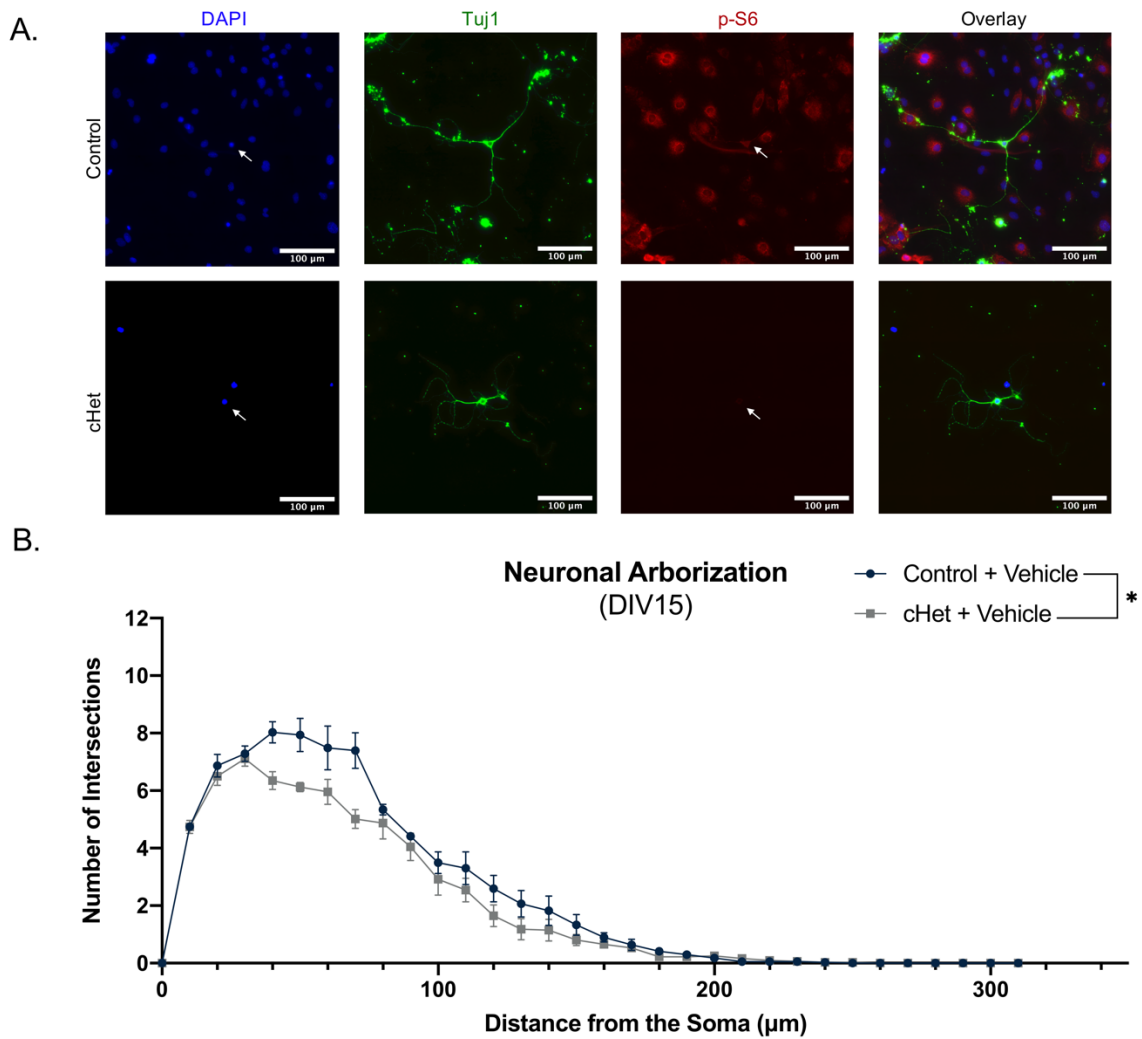


**Figure 6:** Conditional *Dyrk1a* mutant neurons exhibit altered neuronal morphology. **A.** Representative Ctip2 positive cultured neurons at 40X magnification at DIV15. **B.** Sholl analysis of neuronal arborization on individual neurons, n=30-35 from per mouse per genotype. Analyzed by 2-way ANOVA on area under the curve (AUC) from Sholl plot. Two-way ANOVA (genotype and drug) with Tukey's multiple comparisons test on the AUC from the Sholl profile shows a significant interaction between genotype and drug treatment ( $F_{1,8}=5.309$ ,  $P=0.0477$ ). cHet pyramidal neurons exhibit significantly decreased neuronal arborization. Results from *post hoc* tests indicated on graphs. Error bars represent mean +/- SEM. \* $P<0.05$ , \*\* $p<0.01$ , \*\*\* $p<0.001$ , \*\*\*\* $p<0.0001$ .

In order to better understand how ASD deficits are shaped by regulation of neuronal subsets responsible for functional connectivity in the brain, this study focused specifically on layer V pyramidal neurons, as indicated by neuronal enrichment of Ctip2. Layer V pyramidal neurons, the largest neurons of the cortex, are heavily dependent on mTOR signaling to maintain their size (Bekkers, 2011). Layer V pyramidal neurons project subcortically (Hubener & Bolz, 1988), and hence are chiefly responsible for behavior modulation of the cerebral cortex and medial prefrontal cortex to basolateral amygdala (mPFC-BLA) circuitry, both of which are implicated in the processing of social information (Adolphs, 2003). Thus, this data likely has functional implications and may serve as a cellular explanation for the observed behavioral abnormalities observed in *DYRK1A*-associated ASD and related disorders.

#### Sholl analysis of cHet versus control neurons after treatment with (1-3)IGF-1

Primary neuronal culture also enables the rapid testing of potential drugs. In this investigation, neurons were treated with the active peptide (1-3)IGF-1 following a previously described protocol shown to upregulate IGF-1 in culture (Rangasamy et al., 2016). Sholl analysis of individual cultured neurons treated with (1-3)IGF-1 (**Figure 7A**) indicates that the deficits in neurite arborization of conditional *Dyrk1a* cHet mice were fully rescued by drug treatment (**Figure 7B**). A 3-way ANOVA (genotype, drug, and distance) with Sidak's multiple comparisons test show a significant interaction between genotype, drug treatment, and measurement ( $F_{31,256}=1.603$ ,  $P=0.0268$ ). Sholl profiles of both control and cHet mice in treated and untreated conditions are shown together in **Figure 8A** with AUC plot in **Figure 8B**.

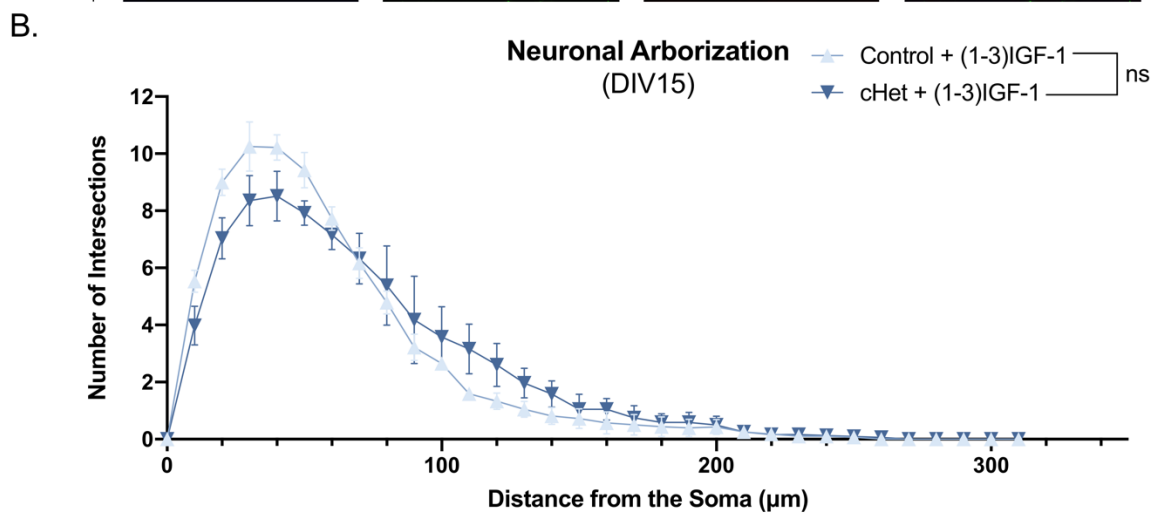
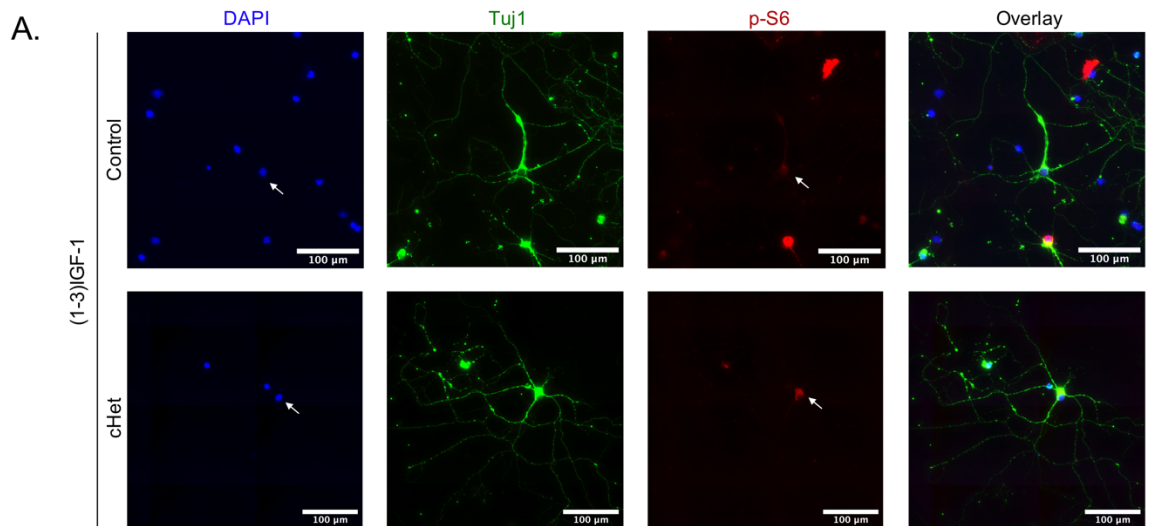


**Figure 7:** Neuronal morphology of conditional *Dyrk1a* mutant neurons can be rescued by (1-3)IGF-1. **A.** Representative (1-3)IGF-1 treated Ctip2 positive neurons at 40X magnification at DIV15. **B.** Sholl analysis of neuronal arborization on individual neurons, n=30-35 from per mouse per genotype. Analyzed by 2-way ANOVA (genotype and drug) on AUC from Sholl plot. Results from *post hoc* tests indicated on graphs. cHet neuronal morphology can be rescued by treatment with (1-3)IGF-1. Error bars represent mean +/- SEM. ns = no significance. \*P<0.05, \*\*p<0.01, \*\*\*p<0.001, \*\*\*\*p<0.0001.

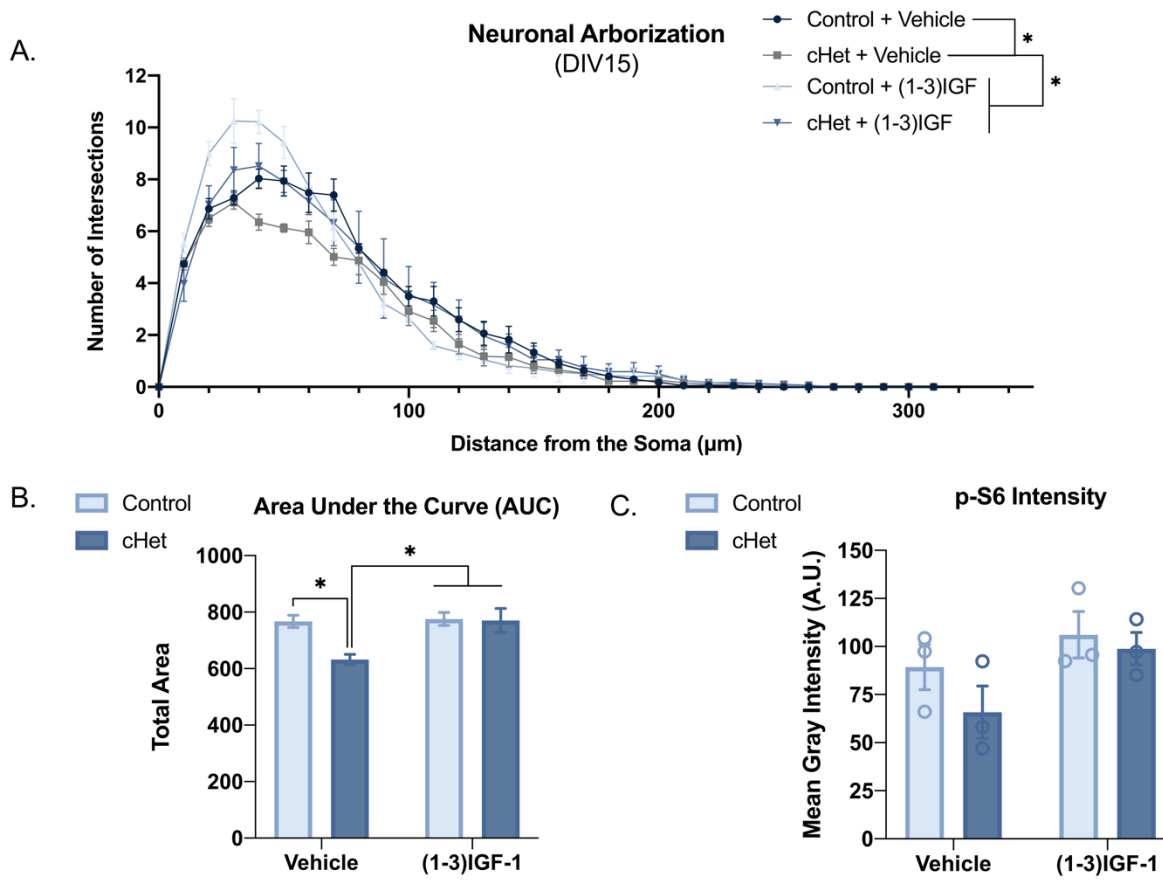


**Figure 8:** *Dyrk1a* cHet neurons display deficits in neuronal morphology that can be rescued by (1-3)IGF-1. **A.** Combined Sholl analysis curves of analyzed neurons at DIV15. Two-way ANOVA (genotype and drug) with Tukey's multiple comparisons test on the AUC from the Sholl profile shows a significant interaction between genotype and drug treatment ( $F_{1,8}=5.457$ ,  $P=0.0477$ ). Three-way ANOVA (genotype, drug, and distance) with Sidak's multiple comparisons test show a significant interaction between genotype, drug treatment, and measurement ( $F_{31,256}=1.603$ ,  $P=0.0268$ ). **B.** Plotted AUC data. **C.** p-S6 intensity as measured by mean grey intensity in arbitrary units (A.U.) showing a decreased mean p-S6 intensity in conditional *Dyrk1a* mutants as compared to control mice and an increased mean p-S6 intensity upon (1-3)IGF-1 treatment for both genotypes. Results from *post hoc* tests indicated on graphs. Error bars represent mean +/- SEM. \* $P<0.05$ , \*\* $p<0.01$ , \*\*\* $p<0.001$ , \*\*\*\* $p<0.0001$ .

### Phosphorylated S6 kinases as a readout of mTOR activity in culture

S6 kinases are directly phosphorylated by mTOR (Ruvinsky et al., 2005). Thus, levels of phosphorylated S6 kinases should be indicative of mTOR activity, which was expected to be downregulated by *Dyrk1a* insufficiency. A plot of p-S6 levels for both genotypes and treatment groups as analyzed by mean grey intensity in arbitrary units (A.U.) is shown in **Figure 8C**. Although the average p-S6 intensity of cHET mice is less than control mice and the averages for both control and cHET mice increase upon (1-3)IGF-1 treatment as expected, the values are not statistically significant. Possible reasons for the lack of significance include a need for a greater sample size, inconsistency of the p-S6 antibody in culture, or microscopy artifacts at 594 nm. This data, given significance, would align with hypothesized downregulation of mTOR signaling in *Dyrk1a* cHET neurons and an upregulation of mTOR signaling as sufficient to rescue *Dyrk1a* mutant phenotype. However, further probing of mTOR signaling in culture would need to be performed in order to confirm this.

### Python code written to automate Sholl analysis

In addition to analyzing the individual neurons exclusively using Fiji ImageJ plugins, a novel Python code was written in order to increase both speed and efficiency of the analysis, as well as gain full control and autonomy over all dataset parameters. The SNT ImageJ plugin was utilized to draw neuronal skeletons, also known as neurite traces, for both ImageJ and Python Sholl methods. The ImageJ method has been documented for future demonstration and use as an ImageJ macro (<tuj1\_p-s6\_workflow.ijm>) and is shown in **Code Appendix A**. A comparison of the workflow for Fiji ImageJ versus novel Python code is shown in **Supplementary Figure 1**.

To summarize the ImageJ portion of the Python workflow, a <.tif> image file of a single Ctip2 positive neuron is imported to Fiji ImageJ (Schindelin et al., 2012) and the three channels contained within it are split (Green = 488 nm, Red = 594 nm, and Blue = 561 nm). Using the freehand drawing tool, a region of interest (ROI) is drawn tightly around the soma of the neuron in the green channel. The neuron is then shuttled into the SNT plugin where, by enabling cursor snapping, all of the neurites emanating from the soma ROI are drawn by hand. Brightness of the image can be adjusted accordingly in order to get a full view of all neurite endings, or terminals. This leads to the most accurate representation of the neuron as possible, especially if the image quality is compromised in certain regions. The neurite traces are then exported as <image.traces> files or <.swc> files. The prior filetype is a compressed XML filetype that can be converted to <.swc> files with the ImageJ Neuroanatomy plugin using the <Convert\_Traces\_to\_SWC.py> Jython script (Ferreira, 2018). The latter filetype is a text file type containing lists of coordinates for points along each of the neurites. Each neurite is exported as a separate <.swc> file. After these files are obtained, the manual portion of the Python workflow is concluded. The Python script then loops over separate folders containing <.tif>, <.roi>, and <.swc> files associated with the individual neurons. These files are batch processed through various modules that open, read, and extrapolate various information for analysis.

The original <.tif> image analyzed in ImageJ is needed to extract information about the shape of the image as a [numpy] array, since the coordinates of the soma and neurites are relative to their position on a specific image. The [ijroi] package can be used to convert <.roi> files into a format that Python can read. The <.swc> file format can be immediately read as a list of connected coordinates. Using this gathered information, the Python code can calculate p-S6 intensity and run Sholl analysis.

Python runs Sholl analysis by essentially looping over the radii of interest, starting at zero and moving at a 10-micron step size, and comparing each radius to a list of distances between every point along a neurite and the center of the soma ROI. If the radius of comparison falls in between the distance value and the next consecutive distance value in both directions, then an intersection is recorded. For a mathematical illustration of this concept, please see **Supplementary Figure 2**. The complexity of Sholl analysis can be broken down into a relatively simple computational problem. The final data generated by the Python code is averaged and neatly exported to a Microsoft Excel spreadsheet. This Python code <tuj1\_p-s6\_workflow.ipynb> as written in Jupyter Notebook can be found in **Code Appendix B**. A comparison of the output from ImageJ versus Python is shown in **Supplementary Figure 3**.

Although the workflows of the two methods diverge (**Supplemental Figure 1**), there are only minor differences between the outputs (**Supplemental Figure 3**). These discrepancies can be explained by distinct differences in ImageJ versus Python. Firstly, the definitions of where coordinates fall relative to a square pixel differs slightly between ImageJ-specific and Python-specific image analysis methods. A deeper explanation of contour tracing with Python [opencv] versus ImageJ has been described in detail (BankHead, 2018). Secondly, since the ImageJ analysis involves the rendering of a binary thresholded image from the neurite trace, there are some issues distinguishing between overlapping neurites. For instance, if two neurites happen to overlap before branching out in different directions, Fiji ImageJ would only be able to count one intersection prior to the fork. On the contrary, Python would be able to detect both neurites prior to the fork, since Python views the neurites as separate lists of coordinates. Please see **Supplementary Figure 4** for a graphical representation of this occurrence. Despite these differences between the two methods, the final data is only subtly varied. Since image analysis is generally associated with error from

drawing ROIs and tracing neurites by hand in addition to other qualitative parameters, the differences between the outputs of these methods are relatively negligible by comparison.

Analysis of the data presented here with the novel Python code produces very similar results to those shown in **Figures 6-8**. Two-way ANOVA (genotype and drug) on AUC data from Sholl plot obtained from Python with Tukey's multiple comparisons test shows significant interaction between genotype and drug treatment ( $F_{1,8}=6.512, P=0.0341$ ). It is likely that the P-value decreases with Python analysis due to the distinction between overlapping neurites as previously described.

## Conclusion

The aims of this investigation were as follows: characterize the effects of *Dyrk1a* conditional mutation on neurite arborization of primary cortical neurons, rescue the effects of *Dyrk1a* mutant phenotype with (1-3)IGF-1 treatment, and develop a novel Python code to automate neurite analysis. In this study, primary cortical neurons were cultured from a *Dyrk1a* mouse model of autism and deficits in neurite arborization were characterized via Sholl analysis in *Dyrk1a* mutants before and after treatment with (1-3)IGF-1. Additionally, a novel Python code was written to automate Sholl analysis.

This study demonstrates how neurons cultured from *Dyrk1a* conditional heterozygous mice exhibit neurite underdevelopment as characterized by decreased neurite complexity. Candidate therapy (1-3)IGF-1, a known mediator of the mTOR signaling cascade, was able to rescue the *Dyrk1a* mutant phenotype. Thus, (1-3)IGF-1 may be a potential therapeutic for patients with *DYRK1A* mutations or related disorders in which mTOR signaling is downregulated.

Additionally, this study introduces a novel method with which to run Sholl analysis and analyze neurite arborization. The Python code described here greatly reduces the number of manual steps associated with using the ImageJ Sholl plugin on an image in addition to accounting for errors otherwise associated with running Sholl analysis on a binary image file.

### **Future Work**

The purpose of this research is to provide a deeper understanding of how autism risk genes, *PTEN* and *DYRK1A*, may converge on mTOR signaling to regulate neuronal development and how dysregulation shapes ASD deficits. Thus, future studies will utilize the methods outlined here to analyze germline heterozygous *Pten* mice. *Pten* data will be compared to the proposed *Dyrk1a* studies in order to contrast how the interplay of both risk genes affects mTOR signaling-regulated neurite growth to shape the etiologies of ASD. Hence, this study serves as a foundational investigation of *Pten* and *Dyrk1a* associated effects on the mTOR growth signaling pathway. *Dyrk1a* cultures may also be used to test other drug-like compounds that act on mTOR signaling, such as a GSK3 $\beta$  inhibitor, to attempt rescue of *Dyrk1a* mutant phenotype. Furthermore, the strategy and code described here may be used to study the intersections of various neurodevelopmental risk genes across a broad array of signaling cascades.

## References

- Abekhoukh, S., Planque, C., Ripoll, C., Urbaniak, P., Paul, J.-L., Delabar, J.-M., & Janel, N. (2013). Dyrk1A, a Serine/Threonine Kinase, is Involved in ERK and Akt Activation in the Brain of Hyperhomocysteinemic Mice. *Molecular Neurobiology*, 47(1), 105-116. doi:10.1007/s12035-012-8326-1
- Adolphs, R. (2003). Cognitive neuroscience of human social behaviour. *Nature Reviews Neuroscience*, 4(3), 165-178. doi:10.1038/nrn1056
- American Psychiatric Association., & American Psychiatric Association. DSM-5 Task Force. (2013). *Diagnostic and statistical manual of mental disorders : DSM-5* (5th ed.). Washington, D.C.: American Psychiatric Association.
- Arbones, M. L., Thomazeau, A., Nakano-Kobayashi, A., Hagiwara, M., & Delabar, J. M. (2019). DYRK1A and cognition: A lifelong relationship. *Pharmacol Ther*, 194, 199-221. doi:10.1016/j.pharmthera.2018.09.010
- Arranz, J., Balducci, E., Arato, K., Sanchez-Elexpuru, G., Najas, S., Parras, A., . . . Arbones, M. L. (2019). Impaired development of neocortical circuits contributes to the neurological alterations in DYRK1A haploinsufficiency syndrome. *Neurobiol Dis*, 127, 210-222. doi:10.1016/j.nbd.2019.02.022
- Baio, J., Wiggins, L., Christensen, D. L., Maenner, M. J., Daniels, J., Warren, Z., . . . Dowling, N. F. (2018). Prevalence of Autism Spectrum Disorder Among Children Aged 8 Years - Autism and Developmental Disabilities Monitoring Network, 11 Sites, United States, 2014. *MMWR Surveill Summ*, 67(6), 1-23. doi:10.15585/mmwr.ss6706a1

- Ballard, F. J., Wallace, J. C., Francis, G. L., Read, L. C., & Tomas, F. M. (1996). Des(1-3)IGF-I: a truncated form of insulin-like growth factor-I. *Int J Biochem Cell Biol*, 28(10), 1085-1087. doi:10.1016/1357-2725(96)00056-8
- Bang, P., Polak, M., Woelfle, J., Houchard, A., & Group, E. I. R. S. (2015). Effectiveness and Safety of rhIGF-1 Therapy in Children: The European Increlex(R) Growth Forum Database Experience. *Horm Res Paediatr*, 83(5), 345-357. doi:10.1159/000371798
- BankHead, P. (2018). Notes on contours. Retrieved from <https://petebankhead.github.io/qupath/technical/2018/03/13/note-on-contours.html>
- Becker, W., & Sippl, W. (2011). Activation, regulation, and inhibition of DYRK1A. *FEBS J*, 278(2), 246-256. doi:10.1111/j.1742-4658.2010.07956.x
- Bekkers, J. M. (2011). Pyramidal neurons. *Curr Biol*, 21(24), R975. doi:10.1016/j.cub.2011.10.037
- Castro, J., Garcia, R. I., Kwok, S., Banerjee, A., Petracic, J., Woodson, J., . . . Sur, M. (2014). Functional recovery with recombinant human IGF1 treatment in a mouse model of Rett Syndrome. *Proc Natl Acad Sci U S A*, 111(27), 9941-9946. doi:10.1073/pnas.1311685111
- Chen, Y., Huang, W.-C., Séjourné, J., Clipperton-Allen, A. E., & Page, D. T. (2015). Pten Mutations Alter Brain Growth Trajectory and Allocation of Cell Types through Elevated  $\beta$ -Catenin Signaling. *The Journal of neuroscience : the official journal of the Society for Neuroscience*, 35(28), 10252-10267. doi:10.1523/JNEUROSCI.5272-14.2015
- Cloetta, D., Thomanetz, V., Baranek, C., Lustenberger, R. M., Lin, S., Oliveri, F., . . . Ruegg, M. A. (2013). Inactivation of mTORC1 in the developing brain causes microcephaly and

affects gliogenesis. *The Journal of neuroscience : the official journal of the Society for Neuroscience*, 33(18), 7799-7810. doi:10.1523/JNEUROSCI.3294-12.2013

Corvin, A. P., Molinos, I., Little, G., Donohoe, G., Gill, M., Morris, D. W., & Tropea, D. (2012).

Insulin-like growth factor 1 (IGF1) and its active peptide (1-3)IGF1 enhance the expression of synaptic markers in neuronal circuits through different cellular mechanisms. *Neurosci Lett*, 520(1), 51-56. doi:10.1016/j.neulet.2012.05.029

Courcet, J. B., Faivre, L., Malzac, P., Masurel-Paulet, A., Lopez, E., Callier, P., . . . Thauvin-Robinet, C. (2012). The DYRK1A gene is a cause of syndromic intellectual disability with severe microcephaly and epilepsy. *J Med Genet*, 49(12), 731-736.  
doi:10.1136/jmedgenet-2012-101251

Cully, M., You, H., Levine, A. J., & Mak, T. W. (2006). Beyond PTEN mutations: the PI3K pathway as an integrator of multiple inputs during tumorigenesis. *Nat Rev Cancer*, 6(3), 184-192. doi:10.1038/nrc1819

Dang, T., Duan, W. Y., Yu, B., Tong, D. L., Cheng, C., Zhang, Y. F., . . . Wu, B. L. (2018). Autism-associated Dyrk1a truncation mutants impair neuronal dendritic and spine growth and interfere with postnatal cortical development. *Molecular psychiatry*, 23(3), 747-758.  
doi:10.1038/mp.2016.253

Ferreira, T. (2018). Convert Traces to SWC. Retrieved from

[https://github.com/tferr/hIPNAT/blob/master/src/main/resources/scripts/Plugins/NeuroAnatomy/Convert\\_Traces\\_to\\_SWC.py](https://github.com/tferr/hIPNAT/blob/master/src/main/resources/scripts/Plugins/NeuroAnatomy/Convert_Traces_to_SWC.py)

Fotaki, V., Dierssen, M., Alcántara, S., Martínez, S., Martí, E., Casas, C., . . . Arbonés, M. L. (2002). Dyrk1A haploinsufficiency affects viability and causes developmental delay and

abnormal brain morphology in mice. *Molecular and cellular biology*, 22(18), 6636-6647.

doi:10.1128/mcb.22.18.6636-6647.2002

Frazier, T. W., Embacher, R., Tilot, A. K., Koenig, K., Mester, J., & Eng, C. (2015). Molecular and phenotypic abnormalities in individuals with germline heterozygous PTEN mutations and autism. *Molecular psychiatry*, 20(9), 1132-1138. doi:10.1038/mp.2014.125

Geschwind, D. H. (2008). Autism: many genes, common pathways? *Cell*, 135(3), 391-395.

doi:10.1016/j.cell.2008.10.016

Gorski, J. A., Talley, T., Qiu, M., Puelles, L., Rubenstein, J. L., & Jones, K. R. (2002). Cortical excitatory neurons and glia, but not GABAergic neurons, are produced in the Emx1-expressing lineage. *The Journal of neuroscience : the official journal of the Society for Neuroscience*, 22(15), 6309-6314. doi:20026564

Huang, W.-C., Chen, Y., & Page, D. T. (2016). Hyperconnectivity of prefrontal cortex to amygdala projections in a mouse model of macrocephaly/autism syndrome. *Nature communications*, 7, 13421-13421. doi:10.1038/ncomms13421

Huang, W. C., Chen, Y., & Page, D. T. (2019). Genetic Suppression of mTOR Rescues Synaptic and Social Behavioral Abnormalities in a Mouse Model of Pten Haploinsufficiency. *Autism Res*, 12(10), 1463-1471. doi:10.1002/aur.2186

Hubener, M., & Bolz, J. (1988). Morphology of identified projection neurons in layer 5 of rat visual cortex. *Neurosci Lett*, 94(1-2), 76-81. doi:10.1016/0304-3940(88)90273-x

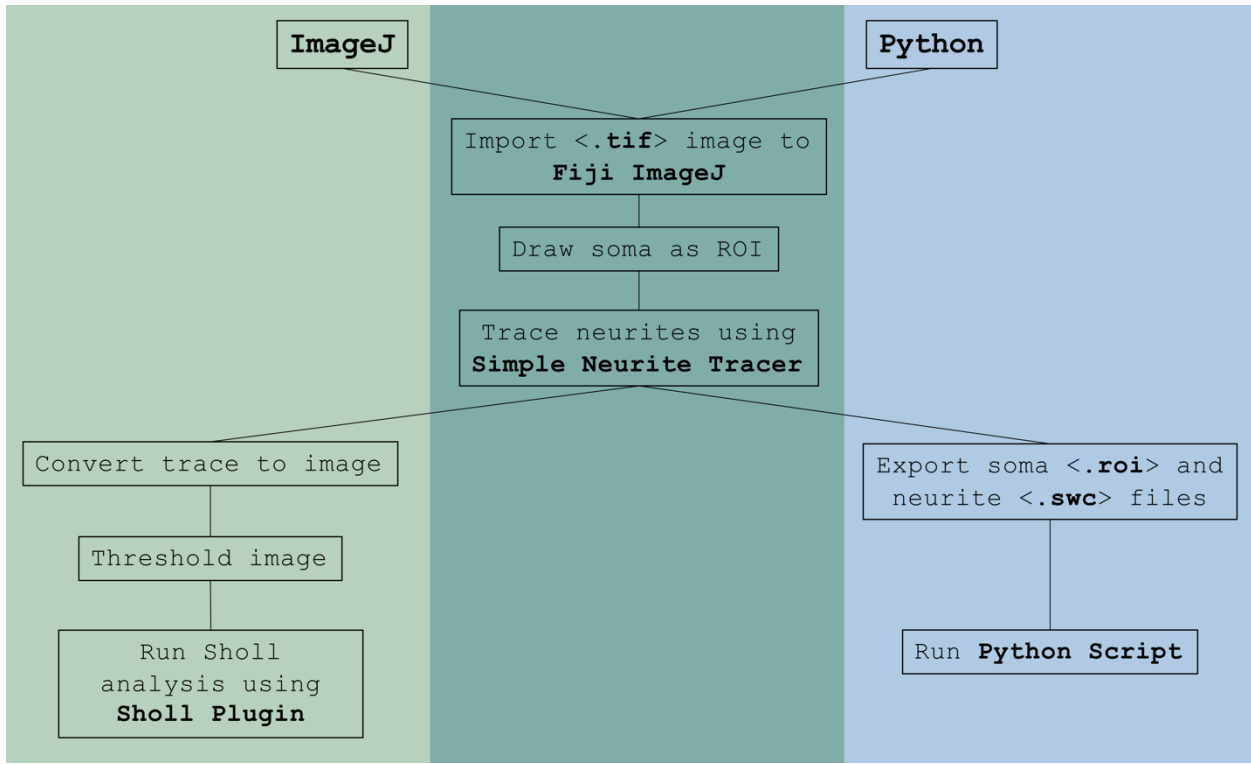
Ji, J., Lee, H., Argiroopoulos, B., Dorrani, N., Mann, J., Martinez-Agosto, J. A., . . . Quintero-Rivera, F. (2015). DYRK1A haploinsufficiency causes a new recognizable syndrome with microcephaly, intellectual disability, speech impairment, and distinct facies. *Eur J Hum Genet*, 23(11), 1473-1481. doi:10.1038/ejhg.2015.71

- Kanner, L. (1943). Autistic disturbances of affective contact. *Nervous Child*, 2, 217-250.
- Laplante, M., & Sabatini, D. M. (2012). mTOR signaling in growth control and disease. *Cell*, 149(2), 274-293. doi:10.1016/j.cell.2012.03.017
- Lipton, J. O., & Sahin, M. (2014). The neurology of mTOR. *Neuron*, 84(2), 275-291. doi:10.1016/j.neuron.2014.09.034
- Ma, X. M., & Blenis, J. (2009). Molecular mechanisms of mTOR-mediated translational control. *Nature Reviews Molecular Cell Biology*, 10(5), 307-318. doi:10.1038/nrm2672
- Martinez de Lagran, M., Benavides-Piccione, R., Ballesteros-Yáñez, I., Calvo, M., Morales, M., Fillat, C., . . . Dierssen, M. (2012). DyRK1A Influences Neuronal Morphogenesis Through Regulation of Cytoskeletal Dynamics in Mammalian Cortical Neurons. *Cerebral Cortex*, 22(12), 2867-2877. doi:10.1093/cercor/bhr362
- Park, H. R., Lee, J. M., Moon, H. E., Lee, D. S., Kim, B. N., Kim, J., . . . Paek, S. H. (2016). A Short Review on the Current Understanding of Autism Spectrum Disorders. *Exp Neurobiol*, 25(1), 1-13. doi:10.5607/en.2016.25.1.1
- Rangasamy, S., Olfers, S., Gerald, B., Hilbert, A., Svejda, S., & Narayanan, V. (2016). Reduced neuronal size and mTOR pathway activity in the MeCP2 A140V Rett syndrome mouse model. *F1000Res*, 5, 2269. doi:10.12688/f1000research.8156.1
- Ratner, M. (2005). New IGF drug stirs competition in growth factor segment. *Nat Biotechnol*, 23(10), 1192. doi:10.1038/nbt1005-1192
- Raveau, M., Shimohata, A., Amano, K., Miyamoto, H., & Yamakawa, K. (2018). DYRK1A-haploinsufficiency in mice causes autistic-like features and febrile seizures. *Neurobiol Dis*, 110, 180-191. doi:10.1016/j.nbd.2017.12.003

- Rosina, E., Battan, B., Siracusano, M., Di Criscio, L., Hollis, F., Pacini, L., . . . Bagni, C. (2019). Disruption of mTOR and MAPK pathways correlates with severity in idiopathic autism. *Transl Psychiatry*, 9(1), 50. doi:10.1038/s41398-018-0335-z
- Ross, M., Francis, G. L., Szabo, L., Wallace, J. C., & Ballard, F. J. (1989). Insulin-like growth factor (IGF)-binding proteins inhibit the biological activities of IGF-1 and IGF-2 but not des-(1-3)-IGF-1. *Biochem J*, 258(1), 267-272. doi:10.1042/bj2580267
- Ruvinsky, I., Sharon, N., Lerer, T., Cohen, H., Stolovich-Rain, M., Nir, T., . . . Meyuhas, O. (2005). Ribosomal protein S6 phosphorylation is a determinant of cell size and glucose homeostasis. *Genes Dev*, 19(18), 2199-2211. doi:10.1101/gad.351605
- Sato, A. (2016). mTOR, a Potential Target to Treat Autism Spectrum Disorder. *CNS Neurol Disord Drug Targets*, 15(5), 533-543. Retrieved from <https://www.ncbi.nlm.nih.gov/pubmed/27071790>
- Saxton, R. A., & Sabatini, D. M. (2017). mTOR Signaling in Growth, Metabolism, and Disease. *Cell*, 169(2), 361-371. doi:10.1016/j.cell.2017.03.035
- Scales, T. M., Lin, S., Kraus, M., Goold, R. G., & Gordon-Weeks, P. R. (2009). Nonprimed and DYRK1A-primed GSK3 beta-phosphorylation sites on MAP1B regulate microtubule dynamics in growing axons. *J Cell Sci*, 122(Pt 14), 2424-2435. doi:10.1242/jcs.040162
- Schindelin, J., Arganda-Carreras, I., Frise, E., Kaynig, V., Longair, M., Pietzsch, T., . . . Cardona, A. (2012). Fiji: an open-source platform for biological-image analysis. *Nat Methods*, 9(7), 676-682. doi:10.1038/nmeth.2019
- Sulis, M. L., & Parsons, R. (2003). PTEN: from pathology to biology. *Trends Cell Biol*, 13(9), 478-483. Retrieved from <https://www.ncbi.nlm.nih.gov/pubmed/12946627>

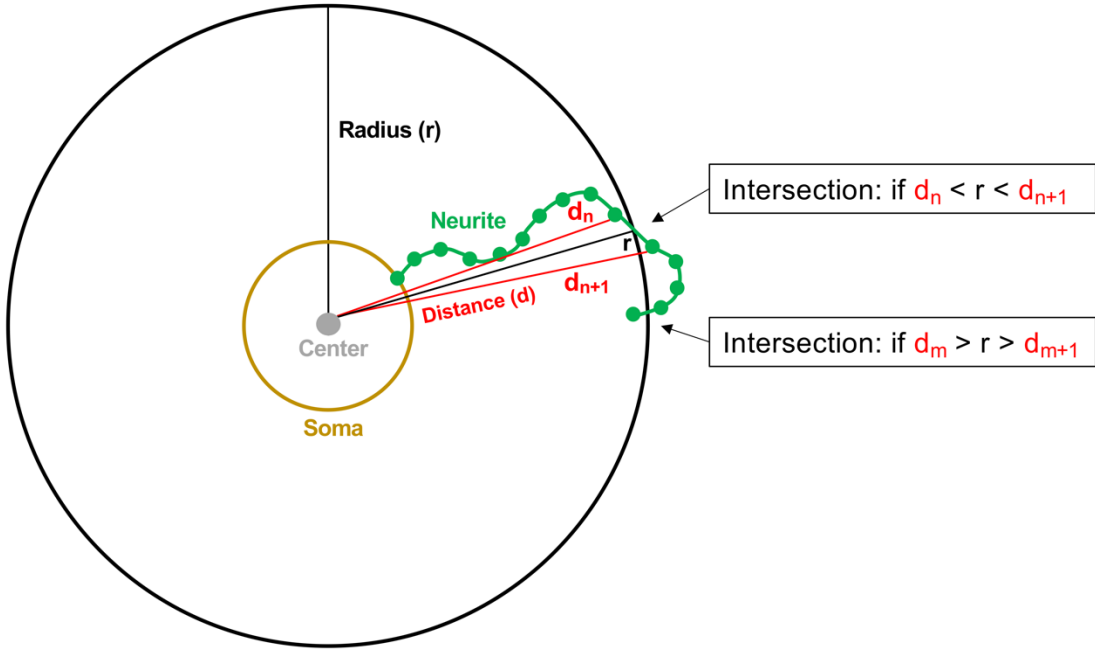
- van Bon, B. W., Coe, B. P., Bernier, R., Green, C., Gerdts, J., Witherspoon, K., . . . Eichler, E. E. (2016). Disruptive de novo mutations of DYRK1A lead to a syndromic form of autism and ID. *Molecular psychiatry*, 21(1), 126-132. doi:10.1038/mp.2015.5
- van Bon, B. W. M., Coe, B. P., de Vries, B. B. A., & Eichler, E. E. (1993). DYRK1A-Related Intellectual Disability Syndrome. In M. P. Adam, H. H. Ardinger, R. A. Pagon, S. E. Wallace, L. J. H. Bean, K. Stephens, & A. Amemiya (Eds.), *GeneReviews(R)*. Seattle (WA).
- Winden, K. D., Ebrahimi-Fakhari, D., & Sahin, M. (2018). Abnormal mTOR Activation in Autism. *Annu Rev Neurosci*, 41, 1-23. doi:10.1146/annurev-neuro-080317-061747
- Wong, M. (2013). Mammalian target of rapamycin (mTOR) pathways in neurological diseases. *Biomed J*, 36(2), 40-50. doi:10.4103/2319-4170.110365

## Supplementary Figures

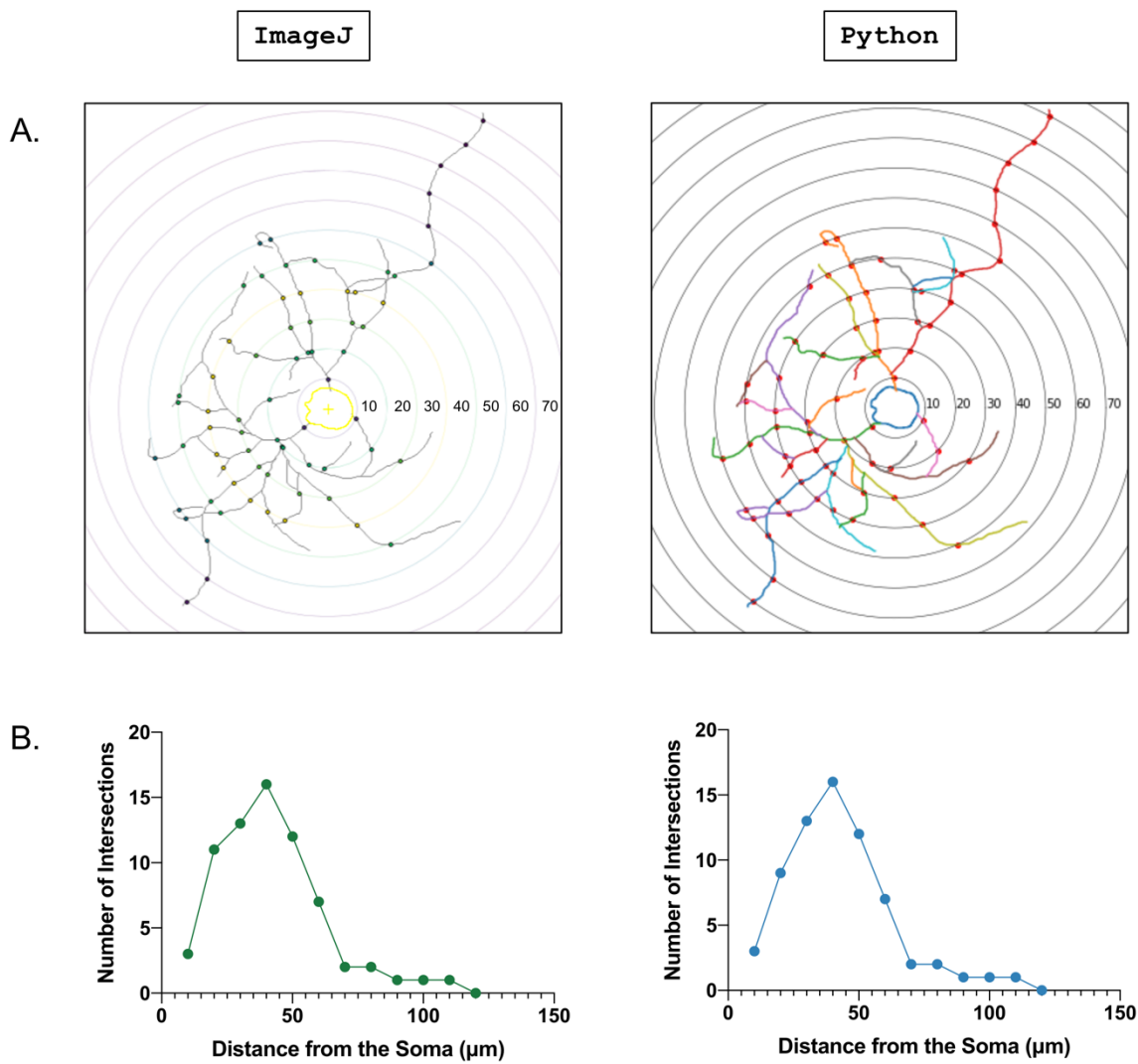


**Supplementary Figure 1:** A comparison of Sholl analysis methods—workflow. Light green: simplified ImageJ workflow. Dark green: overlapping methods. Light blue: simplified Python workflow.

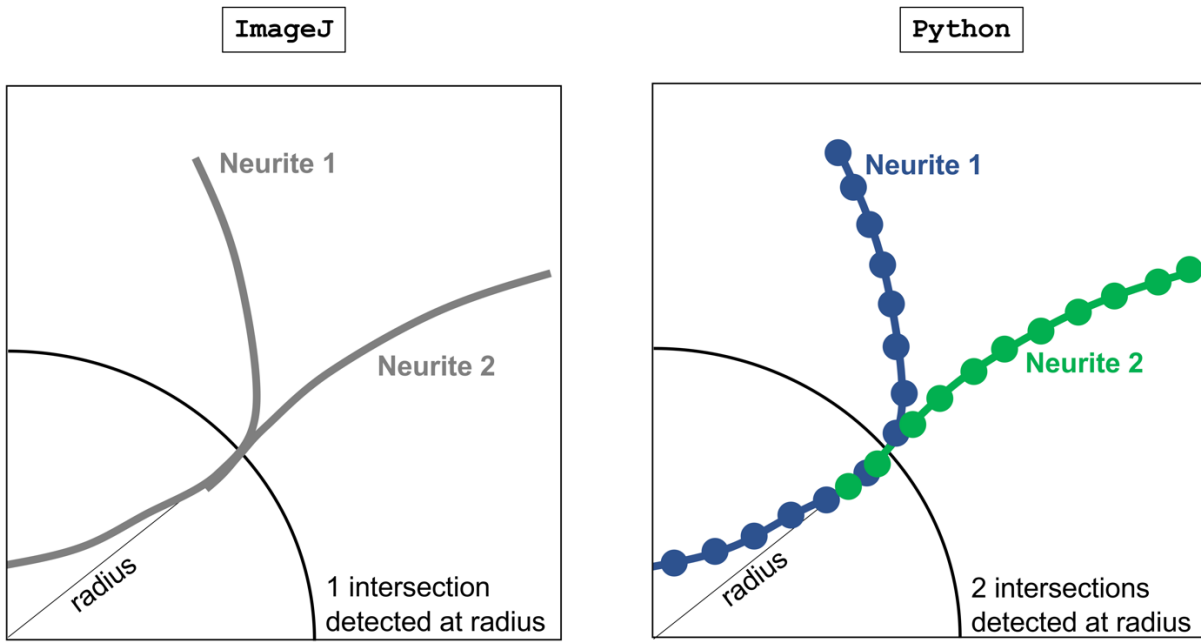
## Sholl Intersections in Python



**Supplementary Figure 2:** Mathematical representation of Sholl intersections in Python. The neuronal trace is drawn emanating from the **soma** ROI in ImageJ SNT. Each **neurite** path is exported as a separate `<.swc>` file that contains a list of connected points. In order to run Sholl analysis, the number of collective intersections between these neurites and circles at given radii from the **center** of the soma must be determined. For simplicity, this schematic illustrates how Python calculates the number of intersections of a single neurite from a single neuron at a given **radius (r)**. Intersections are mathematically determined by comparing the radius ( $r$ ) to **distances** from the center of the soma to the neurite points. If the radius value is greater than distance ( $d_n$ ) and less than the next consecutive distance ( $d_{n+1}$ ) along the neurite, then an intersection is counted. Since neurite terminals can sometimes loop back towards the soma, this comparison must be made in both directions. Thus, if the radius is less than distance ( $d_m$ ) and greater than the next consecutive distance ( $d_{m+1}$ ) along the neurite, an intersection is, likewise, recorded. In this graphical representation, Python would detect a total of two intersections at radius ( $r$ ).



**Supplementary Figure 3:** A comparison of Sholl analysis methods—output. **A.** Example Sholl analysis on an individual example neuron for ImageJ and Python workflows. Neurite traces depicted with radii of concentric circles in  $\mu\text{m}$ . Intersections of neurites with concentric circles shown as dots. ImageJ plot generated by the Sholl analysis plugin and Python plot generated using [matplotlib.pyplot]. **B.** Sholl analysis graphed as a curve. Minimal difference in number of intersections observed at 20  $\mu\text{m}$  distance from the soma. Likely due to contour processing differences between the methods as observed by discrepancies in soma position relative to the concentric circles.



**Supplementary Figure 4:** A comparison of Sholl analysis methods—neurite trace. ImageJ Sholl analysis calculates the number of intersections from a binary image. Python calculates the number of intersections based off of a list of connected points contained in the <.swc> file for each neurite. For an explanation of Python Sholl intersections, please refer to **Supplementary Figure 2**. Thus, Python is always able to detect overlapping neurites.

## Code Appendix

### Code Appendix A: ImageJ Macro (IJM)

```
=====<tuj1_p-s6_workflow.ijm>=====

//This <.ijm> performs Sholl analysis on individual neurons using only Fiji
ImageJ
// Created using ijmacros recorder

// Conversion factor used here is for a VS-120 microscope at 40X magnification
run("Set Scale...", "distance=1 known=0.16094 pixel=1 unit=micron global");

// Draw soma
run("Split Channels");
// setTool("freehand");
waitForUser("Waiting for user to draw a soma in green channel. Press Okay to
continue....");

// Save soma
roiManager("Add");
run("Measure");

// Record p-S6 brightness
waitForUser("Select red channel and press Okay to continue....");
roiManager("Select", 0);
run("Measure");

// Trace neurites in Simple Neurite Tracer (SNT)
waitForUser("Select green channel and press Okay to continue....");
run("Simple Neurite Tracer", "look_for_tubeness look_for_previously_traced");
roiManager("Select", 0);
roiManager("Show All");
waitForUser("Waiting for user to draw a neurites, save trace, obtain summary, and
exit. Press Okay to continue....");

// Run Sholl analysis
waitForUser("Select neurite trace and press Okay to continue....");
setAutoThreshold("Default no-reset");
roiManager("Select", 0);
run("Sholl Analysis (From Image)...");
waitForUser("Waiting for user to set end radius and run Sholl. Press Okay to
close....");
run("Close");

=====
```

## **Code Appendix B:** Python code

===== <tuj1\_p-s6\_workflow.ipynb> =====

Please see following pages.

# tuj1 p-s6 sholl workflow

**Purpose:** organize files, run Sholl analysis, and process data

**Conventions:** image analysis coordinates (row, column) pair

**Note:** this data set (ROI, neurite trace) was acquired in ImageJ set to micron units and will be converted to pixels for analysis in Python

In [1]:

```
import glob
import os
import sys
import shutil
import cv2
import ijroi
import numpy as np
import matplotlib.pyplot as plt
import pandas as pd

# the following conversion factor is specific to a VS-120 microscope 40X objective
p2m = 0.16094 # pixels to micron
```

**Directory setup:** main folder containing directories "code" (current working directory), "data", and "output"

- All code written and stored in "code"
- All data files contained within "data"
- All output exported to "output"

In [2]:

```
'''Check that current working directory is "code"'''

cwd = os.getcwd()
get_cwd = cwd.split('/')
print('Current working directory is:', get_cwd[-1], '\tMain folder:', get_cwd[-2])

# make "data" and "output" directories

if not os.path.exists('../data'):
    os.mkdir('../data')

if not os.path.exists('../output'):
    os.mkdir('../output')
```

Current working directory is: code Main folder: DIV15\_50000\_Tuj1483\_p-S6\_594\_Ctip2\_647\_Veh\_IGF-1

## Directory Hierarchy

This is how the folders need to be structured in order for the code to run. < > indicates a file.

- Main folder
  - code
    - tuj1\_p-S6\_sholl\_workflow.ipynb >
  - data
    - final\_neurons
      - Ms# (e.g. cHET2)
      - treatment (e.g. veh)
        - tag\_neuron\_#
          - SWC
    - output

## Make neuron folders and organize neuron files into folders

In [3]:

```
# create "final_neurons" directory according to directory hierarchy above

if not os.path.exists('../data/final_neurons'):
    os.mkdir('../data/final_neurons')
```

In [4]:

```
'''Place <tag_neuron_#.tif> files of individual neurons into "final_neurons" directory'''

# make folders with same names as the neuron files
for f1 in sorted(glob.glob('../data/*.tif')):
    dot, dot1, name, ext = f1.split('.')
    slash, data, neuron = name.split('/')
    if not os.path.exists('../data/final_neurons/' + neuron):
        os.mkdir('../data/final_neurons/' + neuron)

for f1 in sorted(glob.glob('../data/final_neurons/*')):
    # create directories to store <.swc> files
    if not os.path.exists(f1 + '/swc'):
        os.mkdir(f1 + '/swc')
```

## ImageJ

**IMPORTANT:** These steps should be completed before running the rest of the code.

- 1.) Drag and drop (import) all <.tif> files into Fiji ImageJ
- 2.) Use ijmacro <tuj1\_p-s6\_workflow.ijm> to draw soma ROI and neurites in Simple Neurite Tracer (SNT)
- 3.) Save <.roi/.swc> files to appropriate folders
  - <.roi> file in “tag\_neuron\_#” folder
  - <.swc> file(s) in “swc” folder” (which is located in “tag\_neuron\_#” folder)

## Required Files

Required files for each tag\_neuron\_# directory

1. TIF file of individual neuron: “tag\_neuron\_#.tif”
2. ImageJ ROI file: “\_\_\_\_.roi”
3. SNT files located in swc folder: “\_\_\_\_.swc”

In [5]:

```
# move <.tif> files into "tag_neuron_#" folders
for f1 in sorted(glob.glob('../data/*.tif')):
    f2 = '../data/final_neurons/' + neuron + '/' + neuron + '.' + ext
    # move neuron files into neuron folders
    os.rename(f1,f2)
```

## Make mouse and treatment folders

In [6]:

```
'''Create treatment folders within mouse folders based on directory hierarchy'''

# enter mice separated by a comma (e.g. Ctrl1, cHet2, Ctrl3, cHet4, cHet5, Ctrl6)

mice = input('Enter mice: ')
mice_list = mice.split(',')

for mouse in mice_list:
    if not os.path.exists('../data/final_neurons/' + mouse):
        os.mkdir('../data/final_neurons/' + mouse)

# enter treatment groups separated by a comma (e.g. veh, igf)

treatments = input('Enter treatment groups: ')
treatments_list = treatments.split(',')

for treatment in treatments_list:
    for mouse in mice_list:
        if not os.path.exists('../data/final_neurons/' + mouse + '/' + treatment):
            os.mkdir('../data/final_neurons/' + mouse + '/' + treatment)

# unblind neurons
# manually move "tag_neuron_#" folders into appropriate mouse and treatment folders
```

```
Enter mice: Ctrl1, cHet2, Ctrl3, cHet4, cHet5, Ctrl6
Enter treatment groups: veh, igf
```

## Check for missing or extra files

In [7]:

```
''' Collect the data folders in a spreadsheet.
Organize an excel sheet containing information about missing/extra files. '''

neuron_dirs = glob.glob('../data/final_neurons/*/*/*')

neurons = []
for d in neuron_dirs:

    # check for single tif file
    tif_files = glob.glob(d+'*.tif')
    if len(tif_files)==1:
        tif = tif_files[0].split('/')[-1]
    else:
        tif = len(tif_files)

    # check for single roi file
    roi_files = glob.glob(d+'*.roi')
    if len(roi_files)==1:
        roi = roi_files[0].split('/')[-1]
    else:
        roi = len(roi_files)

    # check for single swc folder
    swc_folder = glob.glob(d+'*swc')
    if len(swc_folder)==1:
        swc = swc_folder[0].split('/')[-1]
    else:
        swc = len(swc_folder)

    neurons.append(d.split('/')[-3:]+[d,tif,roi,swc])

'''Exported spreadsheet contains a list of data folders.
If data folder contains the wrong number of .tif files, .roi files, or swc folders,
the number will appear instead of the name of the file/folder'''

# export to "output" directory
df = pd.DataFrame(neurons, columns=['mouse','treatment','tag', 'folder','tif','roi','swc'])
df.to_excel('../output/check.xlsx')
```

# Run Analysis

Note: if there are misplaced/missing/extraneous files, the code will fail

In [8]:

```
''' Load <.tif> and <.roi> files, loop over <.swc> files, and run Sholl analysis.'''
neuron_dirs = glob.glob('../data/final_neurons/*/*/*')

# define radii for sholl analysis: np.arange(start value, stop value + 1, step size)
radii = np.arange(0,301,10)/p2m # convert to pixels

# create master dictionaries to store data
soma_size = {}
p_s6_intensity = {}
all_neurite_dict = {}
all_sholl_dict = {'radius':radii*p2m} # convert radii from pixels back to micron
all_intersections = []

for neuron_folder in neuron_dirs:

    # load tif file and get shape
    tif_files = glob.glob(neuron_folder + '/*.tif')[0]
    img = cv2.imread(tif_files)
    size = img.shape[:2]

    # load roi file and get center
    roi_files = glob.glob(neuron_folder + '/*.roi')[0]
    with open(roi_files, 'rb') as f:
        roi = ijroi.read_roi(f).T
        cont = roi[::-1].T.reshape(-1,1,2).astype(np.int32)
        img2 = np.zeros(size,dtype=np.int32)
        cv2.drawContours(img2,[cont],-1,1,thickness=-1)
        roi2 = np.nonzero(img2)
        soma_area = img[roi2]

    # store soma size information
    soma_size[neuron_folder] = { 'soma_size_micron': soma_area.shape[0]*(p2m**2),
                                 }

    # store p-s6 intensity (red channel, 594 nm)
    p_s6_intensity[neuron_folder] = { 'p-S6_min' : soma_area[:,2].min(),
                                      'p-S6_mean' : soma_area[:,2].mean(),
                                      'p-S6_max' : soma_area[:,2].max()
                                     }

    center = np.mean(roi2, axis=1)

    # create a list [neurites] containing coordinates of all neurites (row, column)
    # create a list [distances] containing computed distances

    neurites = []
    distances = []

    # load swc files
    swc_folder = neuron_folder + '/swc/*.*swc'
    for swc_file in sorted(glob.glob(swc_folder)):
        data = np.loadtxt(swc_file,usecols=(3,2))/p2m # convert from micron to pixels
        neurites.append(data)
        distance = np.sqrt((data[:,1]-center[1])**2+(data[:,0]-center[0])**2)
        distances.append(distance)

    # calculate the total length of each neurite by summing distances between points

    branch_lengths = []

    for neurite in neurites:
        dr = neurite[1:]-neurite[:-1]
        dl = np.sqrt(dr[:,0]**2+dr[:,1]**2)
        branch_length = np.sum(dl)
        branch_lengths.append(branch_length*p2m)
```

```

# store neurite data
all_neurite_dict[neuron_folder] = {'total_neurite_length': np.sum(branch_lengths),
                                    'mean_neurite_length': np.mean(branch_lengths),
                                    'number_of_branches': len(branch_lengths),
                                    'longest_branch': max(branch_lengths)
                                   }

# create a list [sholl] for number of intersections
# create a list [intersections] of intersection coordinates (row, column)
sholl = []
intersections = []

# run Sholl analysis
for r in radii:
    counter = 0
    for i in range(len(distances)):
        for j in range(len(distances[i])-1):
            if distances[i][j] < r < distances[i][j+1] or distances[i][j] > r > distances[i][j+1]:
                counter += 1
                intersections.append(neurites[i][j])
    sholl.append(counter)
all_sholl_dict[neuron_folder] = sholl
intersections = np.array(intersections)
all_intersections.append(intersections)

```

## Export raw data to excel sheet

In [9]:

```

# export all raw data to excel sheet named "raw_data" located in "output" folder

df = pd.DataFrame([d.split('/')[-3:]+[d] for d in neuron_dirs],
                  columns=['mouse','treatment','tag','folder'])
dss = pd.DataFrame(soma_size).T
dp = pd.DataFrame(p_s6_intensity).T
dn = pd.DataFrame(all_neurite_dict).T
ds = pd.DataFrame(all_sholl_dict)

writer = pd.ExcelWriter('../output/raw_data.xlsx')

# folder path
df.to_excel(writer,sheet_name='neurons')
worksheet = writer.sheets['neurons']
for c in worksheet.columns: # adjust the width of the columns
    worksheet.column_dimensions[c[0].column_letter].width = 15

# soma size
dss.to_excel(writer,sheet_name='soma_size')
worksheet = writer.sheets['soma_size']
for c in worksheet.columns:
    worksheet.column_dimensions[c[0].column_letter].width = 15

# p-s6 intensity
dp.to_excel(writer,sheet_name='p-s6_intensity')
worksheet = writer.sheets['p-s6_intensity']
for c in worksheet.columns:
    worksheet.column_dimensions[c[0].column_letter].width = 15

# neurite data
dn.to_excel(writer,sheet_name='neurite_data')
worksheet = writer.sheets['neurite_data']
for c in worksheet.columns:
    worksheet.column_dimensions[c[0].column_letter].width = 15

# sholl analysis
ds.to_excel(writer,sheet_name='sholl_data')
worksheet = writer.sheets['sholl_data']
for c in worksheet.columns:
    worksheet.column_dimensions[c[0].column_letter].width = 15

writer.save()

```

## Check for potential errors

In [10]:

```
# check for errors (given that no neurons should have intersections at the radius furthest from the soma)

sholl_data = pd.read_excel('../output/raw_data.xlsx',sheet_name='sholl_data',index_col=0).T
x      = sholl_data.iloc[0]
sholl_data = sholl_data.drop('radius')

neuron_count = []
for d in sholl_data.index:
    neuron_count.append(d)

counter = 0
for i in range(len(neuron_count)):
    if sholl_data.iloc[i][30] > 0:
        print('There might be an error with', sholl_data.index[i])
    counter += 1

if len(neuron_count) == counter:
    print('No neurons have intersections at ' + str(radii[-1]*p2m) + ' micron radius.' )
```

No neurons have intersections at 300.0 micron radius.

## Get average of neurons for each mouse + genotype + treatment group

In [11]:

```
# filter data for each mouse + genotype + treatment group

data = pd.read_excel('../output/raw_data.xlsx',sheet_name='sholl_data',index_col=0).T
data = data.drop('radius')

data['mouse'] = [ d.split('/')[-3] for d in data.index ]
data['treatment'] = [ d.split('/')[-2] for d in data.index ]
data['neuron'] = [ d.split('/')[-1] for d in data.index ]

averaged_sholl = {'radius': radii}

for mouse in data['mouse'].unique():
    for treatment in data['treatment'].unique():

        def filter_(row):
            return (row['mouse']==mouse) & (row['treatment']==treatment)

        Y = data[data.apply(filter_,axis=1)].iloc[:, :-3]
        y = Y.mean(axis=0)
        # store data
        averaged_sholl[mouse,treatment] = y

# export data to excel sheet
writer = pd.ExcelWriter('../output/averaged_sholl_data.xlsx')
da = pd.DataFrame(averaged_sholl)
da.to_excel(writer,sheet_name='averaged_sholl')
worksheet = writer.sheets['averaged_sholl']
writer.save()
```

## Plot average of mice for each genotype + treatment group

In [12]:

```
# plot a curve of distance as a function of number of intersections for each genotype + treatment group

data = pd.read_excel('../output/averaged_sholl_data.xlsx',sheet_name='averaged_sholl',index_col=0)
.T
x = data.iloc[0]
data = data.drop('radius')

data['mouse'] = [d.split("')[-4] for d in data.index]
data['treatment'] = [d.split("')[-2] for d in data.index]

final_averaged_sholl = {('radius',''): radii*p2m}

genotypes = set([m[:4] for m in data['mouse']])

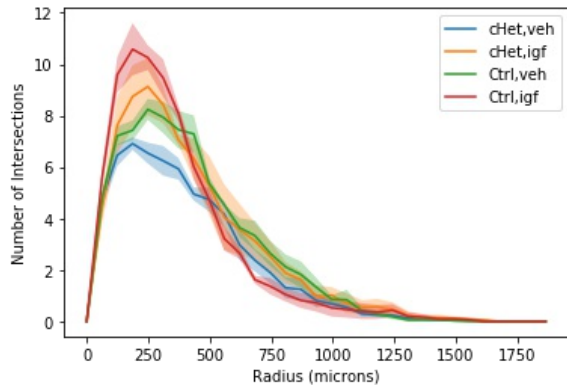
for genotype in genotypes:
    for treatment in data['treatment'].unique():

        def filter_2(row):
            return (row['mouse'][:4]==genotype) & (row['treatment']==treatment)

        Y = data[data.apply(filter_2,axis=1)].iloc[:, :-2]
        y = Y.mean(axis=0)

        # plot averages
        plt.plot(x,y,label=f'{genotype},{treatment}')
        # compute the standard error for this group at each radius.
        # shade between (mean - std error) and (mean + std error).
        dy = Y.sem(axis=0)
        plt.fill_between(x,y-dy,y+dy,alpha=0.3)

# export .tif file of plot
plt.xlabel('Radius (microns)')
plt.ylabel('Number of Intersections')
plt.legend()
plt.savefig("../output/sholl_plot_mice_averages.tif")
plt.show()
```



## Export averaged data to excel sheet

In [13]:

```
# filter all averaged data for each mouse + genotype + treatment group
# save neuron averages for each mouse + genotype + treatment group

def filter_(row):
    return (row['mouse'] == mouse) & (row['treatment'] == treatment)
```

In [14]:

```
# filter and average soma data

data = pd.read_excel('../output/raw_data.xlsx',sheet_name='soma_size',index_col=0)

data['mouse'] = [ d.split('/')[-3] for d in data.index ]
data['treatment'] = [ d.split('/')[-2] for d in data.index ]
data['neuron'] = [ d.split('/')[-1] for d in data.index ]

soma_averages = {}

for mouse in data['mouse'].unique():
    for treatment in data['treatment'].unique():
        Y = data[data.apply(filter_,axis=1)].iloc[:, :-3]
        y = Y.mean(axis=0)
        soma_averages[mouse, treatment] = y
```

In [15]:

```
# filter and average p-s6 data

data = pd.read_excel('../output/raw_data.xlsx',sheet_name='p-s6_intensity',index_col=0)

data['mouse'] = [ d.split('/')[-3] for d in data.index ]
data['treatment'] = [ d.split('/')[-2] for d in data.index ]
data['neuron'] = [ d.split('/')[-1] for d in data.index ]

p_s6_averages = {}

for mouse in data['mouse'].unique():
    for treatment in data['treatment'].unique():
        Y = data[data.apply(filter_,axis=1)].iloc[:, :-3]
        y = Y.mean(axis=0)
        p_s6_averages[mouse, treatment] = y
```

In [16]:

```
# filter and average neurite data

data = pd.read_excel('../output/raw_data.xlsx',sheet_name='neurite_data',index_col=0)

data['mouse'] = [ d.split('/')[-3] for d in data.index ]
data['treatment'] = [ d.split('/')[-2] for d in data.index ]
data['neuron'] = [ d.split('/')[-1] for d in data.index ]

neurite_averages = {}

for mouse in data['mouse'].unique():
    for treatment in data['treatment'].unique():
        Y = data[data.apply(filter_,axis=1)].iloc[:, :-3]
        y = Y.mean(axis=0)
        neurite_averages[mouse, treatment] = y
```

In [17]:

```
# filter and average sholl data

data = pd.read_excel('../output/raw_data.xlsx',sheet_name='sholl_data',index_col=0).T
data = data.drop('radius')

data['mouse'] = [ d.split('/')[-3] for d in data.index ]
data['treatment'] = [ d.split('/')[-2] for d in data.index ]
data['neuron'] = [ d.split('/')[-1] for d in data.index ]

sholl_averages = {'radius': radii*p2m}

for mouse in data['mouse'].unique():
    for treatment in data['treatment'].unique():

        Y = data[data.apply(filter_,axis=1)].iloc[:, :-3]
        y = Y.mean(axis=0)
        sholl_averages[mouse, treatment] = y
```

In [18]:

```
# export averaged data to excel

dsoma = pd.DataFrame(soma_averages)
dps6 = pd.DataFrame(p_s6_averages)
dn = pd.DataFrame(neurite_averages)
dsholl = pd.DataFrame(sholl_averages)

writer = pd.ExcelWriter('../output/averaged_data.xlsx')

dsoma.to_excel(writer,sheet_name='averaged_soma')
worksheet = writer.sheets['averaged_soma']

dps6.to_excel(writer,sheet_name='averaged_p_s6')
worksheet = writer.sheets['averaged_p_s6']

dn.to_excel(writer,sheet_name='averaged_neurite')
worksheet = writer.sheets['averaged_neurite']

dsholl.to_excel(writer,sheet_name='averaged_sholl')
worksheet = writer.sheets['averaged_sholl']

writer.save()
```